A DOUBLE-STREAM AMPLIFIER FOR MICROWAVE FREQUENCIES

By G.A. Harrower

A thesis submitted in partial fulfilment of the requirements for the degree of Master of Science to the Faculty of Graduate Studies and Research, McGill University.

MacDonald Physics Laboratory August 1950

CONTENTS

	Page
ABSTRACT	1
INTRODUCTION	2
MATHEMATICAL THEORY AND DESIGN CALCULATIONS	5
The Conditions Required for Complex L	11
Calculation of Gain	12
Calculation of a Practical Design	16
THE ELECTRON-OPTICAL PROBLEM	17
General Requirements	17
The Rubber Membrane Analogue Method	19
Theory of the Analogue	19
The Apparatus Used	20
The Design of the Electron Gun System	22
Structural Details of the Electron Gun System	27
The Process of Thoria Coating the Cathodes	30
THE CONSTRUCTION OF THE TUBE	31
EXPERIMENTAL MEASUREMENTS	34
General Apparatus	34
Electron-Optical Measurements	35
Radio Frequency Measurements	42
Comparison of Readings Recorded in Table IV	44
Discussion of the Reasons for Energy Losses	47
SUMMARY	49
ACKNOWLEDGEMENTS	52

Page

APPENDIX I

Calculation of Wavelengths in the Electron Streams 53

APPENDIX II

Calculation of Beam Coupling Coefficients 54

APPENDIX III

An Evaluation of Conditions Present in the Tube as Compared with the Theoretical Optimum 55

Calculation of Critical Current Density 55

Calculation of Gain 56

REFERENCES 58

A DOUBLE-STREAM AMPLIFIER FOR MICROWAVE FREQUENCIES

ABSTRACT: The analysis and design of a microwave amplifier tube has been carried out in which amplification is produced by the interaction of two streams of electrons. An electron gun system, able to provide the two streams of electrons, has been built according to observations made on a rubber membrane analogue of the system. Electron-optical tests have verified the behaviour which the analogue method of design predicted. The mechanical construction of the tube is described here in detail. Radio frequency tests made at a signal wavelength of 10.7 cm. have confirmed the existence of the process of double-stream amplification.

INTRODUCTION

In recent years the problem of amplifying high radio frequences has received much attention and several types of tubes have been developed for that purpose. The limitations of transit time and interelectrode capacitances have made the conventional triode useless at high frequencies. This led to the development of the klystron in which the a.c. and d.c. fields are separated so that a very short transit time through the grids of a resonant cavity can be obtained. Amplification in the klystron is due to the increasing wave set up in a velocity modulated stream of electrons. The travelling wave tube produces amplification by means of the interaction of two waves, one existing in a stream of electrons and the other travelling along a wave-guiding structure, usually a helix, surrounding the electron stream. Close synchronism of the two waves must be maintained. In a fourth method, that with which this paper is concerned, the process of amplification occurs in the interaction of two streams of electrons travelling at different velocities and having different current densities. In this double-stream amplifier, amplification takes place independently of any physical structure. The advantage in this is that

no parts of the tube in the amplifying region are limited in size or in power dissipation by the shortness of the signal wavelength.

Some half dozen papers on double-stream amplifiers have been published during the past eighteen months. Two of these describe experimental tubes and the performance which they gave. An article by Haeff (1) at the Naval Research Laboratories, tells of tubes which amplified signals at a frequency of 3000 mc. A paper by Hollenberg (2) at the Bell Telephone Laboratories reports the observation of double-stream amplification at a frequency of 255 mc. Papers concerned with the theory of double-stream amplification include those by Nergaard (3) at R.C.A., and Pierce and Hebenstreit (4) at Bell Telephone. The special analysis necessary when the electron beams are concentric tubular in form, and the presentation of numerical data in graphs to cover a wide range of conditions where double-stream interaction will occur, are presented by Pierce in two other papers, references 5 and 6, respectively. To complete the list of recent papers dealing directly with double-stream amplifiers, there is Hollenberg's account of his experimental work written in a non-technical style without mathematical detail (7).

A brief qualitative description of a double-stream amplifier and the process of amplification may serve as preparation for the quantitative analysis to follow. The amplifier's first requirement is an electron gun system producing two streams of electrons having the proper velocities and current densities and occupying a common cylindrical space. By means of a short helix or a resonant cavity the high frequency signal to be amplified is impressed on the electron beams. This modulation process sets up, in the electron streams, waves which are fluctuations of the space-charge density with corresponding fluctuations of the electric field. Since the two electron streams occupy a common space they interact and the space-charge waves are modified. If conditions are correct there is set up a growing wave which increases exponentially with distance along the length of the tube. Lateral spreading of the electron streams throughout the drift space is prevented by placing the tube in the longitudinal magnetic field of a solenoid. The amplified signal is removed from the electron streams as they pass through a second short helix or resonant cavity. It is to be noted that the amplification occurs in the electron streams themselves. The two important factors in the propagation of the increasing wave are the electric field due to the charge density and the electrons whose mass serves to store kinetic energy.

MATHEMATICAL THEORY AND DESIGN CALCULATIONS

This section deals with an analysis of increasing space-charge waves in two interacting streams of electrons. It is directed toward obtaining values of the various electrical and physical parameters which may be used for the design of a practical device. Of the several approaches to the theory of double-stream amplification already mentioned, this follows most closely that published by Nergaard (3).

Consider two streams of electrons designated by subscripts 1 and 2 moving in a common space in the x direction and infinite in extent in the other two directions. The following symbols will be used:

p = d.c. space-charge density of electrons

r = a.c. space-charge density of electrons

u = d.c. velocity of electrons

v = a.c. velocity of electrons

E = a.c. electric field

$y = \sqrt{\frac{4\pi ep}{m}}$ = plasma frequency

e/m = charge to mass ratio of the electron.

In the equations to follow small signals are assumed so that second order terms may be neglected.

The equation of motion for either beam has the form

$$\text{force} = \text{mass} \times \text{acceleration}$$

which is

$$eE = m\left[\frac{dv}{dt} + \frac{dx}{dt}\frac{dv}{dx}\right]$$

$$= m\left[\frac{dv}{dt} + u\frac{dv}{dx}\right]$$

Thus the two equations of motion are written

$$\frac{dv_1}{dt} + u_1\frac{dv_1}{dx} = \frac{eE}{m} \qquad (1)$$

$$\frac{dv_2}{dt} + u_2\frac{dv_2}{dx} = \frac{eE}{m} \qquad (2)$$

Conservation of charge is expressed by

$$\nabla . J + \frac{dp}{dt} = 0$$

where J is current density and is equivalent to the charge density multiplied by the velocity.[x] Therefore,

---

[x] In terms of the dimensions of these quantities:

$$J = \frac{\text{amp.}}{\text{cm.}^2} = \frac{\text{coulomb}}{\text{sec. cm.}^2} = \frac{\text{coulomb}}{\text{cm}^3}\frac{\text{cm.}}{\text{sec.}} = pv$$

upon differentiating with respect to x to form the divergence, the equations of conservation of charge for the two beams are written:

$$p_1 \frac{dv_1}{dx} + u_1 \frac{dr_1}{dx} + \frac{dr_1}{dt} = 0 \qquad (3)$$

$$p_2 \frac{dv_2}{dx} + u_2 \frac{dr_2}{dx} + \frac{dr_2}{dt} = 0 \qquad (4)$$

Finally, the interaction between the two electron beams is introduced in the relation

$$\text{div } E = 4\pi (r_1 + r_2) \qquad (5)$$

which states that the a.c. electric field is produced by the total a.c. charge density of the two beams.

Next, assume that all a.c. quantities are periodic in time as exp jwt and in space as exp jLx where L is 2π/wavelength, so that the a.c. quantities may be written:

$$v_1 = v_1 \exp j(wt + Lx)$$

$$v_2 = v_2 \exp j(wt + Lx)$$

$$r_1 = r_1 \exp j(wt + Lx)$$

$$r_2 = r_2 \exp j(wt + Lx)$$

These forms can be substituted into equations 1 to 5. After cancellation of the term $\exp i(wt + Lx)$ throughout, the resulting equations are

From (1) $$j(wt + Lu_1)v_1 = eE/m \tag{6}$$

From (2) $$j(wt + Lu_2)v_2 = eE/m \tag{7}$$

From (3) $$Lp_1v_1 + (w + Lu_1)r_1 = 0 \tag{8}$$

From (4) $$Lp_2v_2 + (w + Lu_2)r_2 = 0 \tag{9}$$

From (5) $$jLE = 4\pi(r_1 + r_2) \tag{10}$$

Equations 6, 7, 8, 9, 10 are five equations in five unknowns: v_1, v_2, r_1, r_2, E. The condition that a solution exist is that the determinant of the coefficients of these five variables should equal zero. That is

$$\begin{vmatrix} j(w + Lu_1) & 0 & 0 & 0 & -e/m \\ 0 & j(w + Lu_2) & 0 & 0 & -e/m \\ Lp_1 & 0 & (w + Lu_1) & 0 & 0 \\ 0 & Lp_2 & 0 & (w + Lu_2) & 0 \\ 0 & 0 & 4\pi & 4\pi & -jL \end{vmatrix} = 0$$

This determinant can be expanded in terms of the elements in the first row and their minors to obtain

$$j(w + Lu_1)\begin{vmatrix} j(w + Lu_2) & 0 & 0 & -e/m \\ 0 & (w + Lu_1) & 0 & 0 \\ Lp_2 & 0 & (w + Lu_2) & 0 \\ 0 & 4\pi & 4\pi & -jL \end{vmatrix}$$

$$-e/m\begin{vmatrix} 0 & j(w + Lu_2) & 0 & 0 \\ Lp_1 & 0 & (w + Lu_1) & 0 \\ 0 & Lp_2 & 0 & (w + Lu_2) \\ 0 & 0 & 4\pi & 4\pi \end{vmatrix} = 0$$

Now expand the first determinant about the element in its second row and the second determinant about the element in its first row to obtain

$$j(w + Lu_1)^2\begin{vmatrix} j(w + Lu_2) & 0 & -e/m \\ Lp_2 & (w + Lu_2) & 0 \\ 0 & 4\pi & -jL \end{vmatrix}$$

$$+j(w + Lu_2)\ e/m\begin{vmatrix} Lp_1 & w + Lu_1 & 0 \\ 0 & 0 & (w + Lu_2) \\ 0 & 4\pi & 4\pi \end{vmatrix} = 0$$

This now reduces directly to

$$j(w + Lu_1)^2 \left[L(w + Lu_2)^2 - 4\pi \; Lp_2 \; e/m \right]$$

$$+j(w + Lu_2) \; e/m \left[-4\pi \; Lp_1 \; (w + Lu_2) \right] \quad = 0$$

$$jL(w + Lu_1)^2 \; (w + Lu_2)^2 - 4\pi \; jLp_2(w + Lu_1)^2 \; e/m$$

$$-4\pi \; jLp_1(w + Lu_2)^2 \; e/m \; = \; 0$$

Cancel the jL factor throughout and substitute the expressions for plasma frequencies

$$y_1^2 \; = \; 4\pi \; p_1 \; e/m \quad \text{and} \quad y_2^2 \; = \; 4\pi \; p_2 \; e/m$$

to obtain

$$(w + Lu_1)^2 \; (w + Lu_2)^2 - y_2^2 \; (w + Lu_1)^2$$

$$-y_1^2 \; (w + Lu_2)^2 \; = \; 0$$

Divide through by the first term and the result is

$$1 \; = \left[\frac{y_1}{w + Lu_1} \right]^2 \; + \; \left[\frac{y_2}{w + Lu_2} \right]^2 \qquad (11)$$

This is a quartic equation in L giving the four values of L for which solutions of the simultaneous equations 1, 2, 3, 4, 5 may exist.

There are three possibilities for the roots of the quartic equation and each has a different physical interpretation. First, if two roots are zero and two real, the situation is that of a conventional velocity modulation tube. Second, if all four roots are real, the action is that of a complex velocity modulation tube. Third, if two of the roots of the quartic in L are complex conjugates

$$L = L_r + jL_i$$

the expression for a.c. electric field

$$E = E \exp j(wt + Lx)$$

becomes

$$E = E \exp j\left[wt + (L_r \pm jL_i)x\right]$$

$$= E \exp j\,(wt + L_r x)\, \exp(\mp L_i x)$$

The factor $\exp L_i x$ represents a growing wave increasing exponentially with distance x .

The Conditions Required for Complex L

It has been shown that a growing wave will exist when the quartic equation in L has a complex root. Nergaard (3) has produced a solution of the quartic and has determined the conditions for complex L. The possible

values of L are formulated in terms of two quantities A and B.

$$A = \frac{\sqrt{y_1 y_2}}{ws} \quad \text{and} \quad B = \sqrt{\frac{y_1}{u_1}\,\frac{u_2}{y_2}}$$

$$\text{where} \quad s = \frac{1}{2}\left(\sqrt{u_1/u_2} - \sqrt{u_2/u_1}\right).$$

$$\text{Also} \quad C = 2/3\left[1 - A^2(B^2 + 1/B^2)/4\right].$$

The condition for a complex root L to exist is

$$A^4 > 2C^3 \tag{12}$$

Calculation of Gain

The gain per unit distance which will occur in such a growing wave can be calculated. In general

gain/unit distance = P(x + 1) / P(x)

where the symbol P stands for power. Power is proportional to EE^x where the ^{x} denotes the complex conjugate. To evaluate EE^x recall that

$$E = E \exp(L_i x) \exp j(wt + L_r x)$$

$$= E \exp(L_i x)\left[\cos(wt + L_r x) + j \sin(wt + L_r x)\right]$$

Therefore,

$$E^x = E \exp(L_i x)\left[\cos(wt + L_r x) - j \sin(wt + L_r x)\right]$$

Thus the product is written

$$EE^x = E^2 \exp(2L_i x)\left[\cos^2(wt + L_r x) + \sin^2(wt + L_r x)\right]$$

Gain per unit length can now be given as

$$G = \frac{P(x+1)}{P(x)} = \frac{E(x+1)\,E^{X}(x+1)}{E(x)\,E^{X}(x)}$$

$$= \frac{\exp 2L_i(x+1)}{\exp(2L_i x)} = \exp(2L_i)$$

Expressed in decibels the gain is

$$G = 10 \log_{10}(\exp 2L_i) = 10 \times 0.4343 \times 2L_i$$

$$= 8.686\ L_i \text{ db./cm.}$$

(having used $\log_{10} Q = 0.4343 \log_e Q$).

The gain is shown by Nergaard (3) to be proportional to a gain factor

$$X = L_i \sqrt{u_1\ u_2 / y_1\ y_2}$$

which has a maximum value of 0.5 when $A = 2/\sqrt{3}$ and $B = 1$.

Thus the expression for gain per unit length becomes

$$G = 8.686\ X \sqrt{y_1\ y_2\ /\ u_1\ u_2} \quad \text{db./cm.} \qquad (13)$$

For convenience in design calculations this expression for G is to be rewritten in terms of practical units with the aid of the relation

$$\frac{y_n}{u_n} = 309 \sqrt{\frac{j_n}{V_n^{3/2}}} \qquad (n = 1, 2) \qquad (14)$$

where j_n = current density in amperes per square centimetre.

V_n = beam velocity in volts.

The optimum values of $A = 2/\sqrt{3}$ and $B = 1$ and the maximum value $X = 0.5$ will be inserted. The relation

$$B = \sqrt{\frac{y_1\ u_2}{u_1\ y_2}} = \sqrt{\frac{j_1}{j_2}\ \left(\frac{V_2}{V_1}\right)^{3/2}} = 1$$

discloses that

$$\sqrt{\frac{j_2}{V_2^{3/2}}} = \frac{1}{B}\sqrt{\frac{j_1}{V_1^{3/2}}} = \sqrt{\frac{j_1}{V_1^{3/2}}}$$

and therefore,

$$\frac{j_2}{V_2^{3/2}} = \frac{j_1}{V_1^{3/2}} \qquad (15)$$

Consequently, the expression for G may now be written

$$G = 8.686 \times 0.5 \sqrt{309\ \sqrt{\frac{j_1}{V_1^{3/2}}}\quad 309\ \sqrt{\frac{j_2}{V_2^{3/2}}}}$$

$$= 1340 \sqrt{\frac{j_1}{V_1^{3/2}}} \qquad \text{db./cm.} \qquad (16)$$

The Ratio of Beam Voltages

The quantity A was defined as

$$\frac{\sqrt{y_1\ y_2}}{ws} = \frac{2\sqrt{y_1\ y_2}}{w\left(\sqrt{u_1/u_2} - \sqrt{u_2/u_1}\right)}$$

In terms of the beam voltages

$$A = \frac{2\ (y_1\ y_2)^{1/2}}{w\left[(V_1/V_2)^{1/4} - (V_2/V_1)^{1/4}\right]}$$

$$= \frac{2\ (y_1\ y_2)^{1/2}}{w\ (V_2/V_1)^{1/4}\left[(V_1/V_2)^{1/2} - 1\right]}$$

$$= \frac{2\ (y_1\ y_2)^{1/2}}{w\ (u_2/u_1)^{1/2}\left[(V_1/V_2)^{1/2} - 1\right]}$$

$$= \frac{2\ (y_1\ y_2)^{1/2}\ \ (y_1/y_2)^{1/2}}{w\ (u_2\ y_1/u_1\ y_2)^{1/2}\left[(V_1/V_2)^{1/2} - 1\right]}$$

$$= \frac{2\ y_1}{wB\left[(V_1/V_2)^{1/2} - 1\right]}$$

For y_1 in terms of practical units write

$$y_1 = 1.85 \times 10^{10} \sqrt{\frac{j_1}{V_1^{1/2}}} \qquad (17)$$

where j_1 = current density in amperes per square centimeter.

V_1 = beam velocity in volts.

Consequently,

$$(V_1/V_2)^{1/2} - 1 = \frac{3.70 \times 10^{10}}{wAB} \sqrt{\frac{j_1}{V_1^{1/2}}}$$

If the optimum values $A = 2/3$ and $B = 1$ are used the final result is

$$(V_1/V_2)^{1/2} - 1 = \frac{3.20 \times 10^{10}}{w} \sqrt{\frac{j_1}{V_1^{3/2}}} \qquad (18)$$

Calculation of a Practical Design

The design of a double-stream amplifier using practical values of voltages and current may now be worked out. Consider the possibility of using a voltage of 400 volts and a current density of 30 ma./cm.^{2} for the faster of the two electron beams. The signal frequency is chosen as 2800 mc. (wavelength 10.7 cm.) which is 1.76×10^{10} radians/sec.

The voltage ratio of the two streams may be calculated from equation 18:

$$\sqrt{\frac{V_1}{V_2} - 1} = \frac{3.20}{1.76} \sqrt{\frac{3 \times 10^{-2}}{20}} = 0.0705$$

Therefore,

$$\frac{V_1}{V_2} = 1.145 \qquad (19)$$

and the voltage of the slower beam is

$$V_2 = 349 \text{ volts.} \tag{20}$$

The value of current density required in the slower beam may be determined from equation 15

$$j_2/V_2^{3/2} = j_1/V_1^{3/2}$$

which was based on the fact that $B = 1$.

Thus $$j_2 = j_1(V_2/V_1)^{3/2} = 24.5 \text{ ma./cm.}^2 \tag{21}$$

The gain per unit length which may be expected is found from equation 16 as

$$G = 1340\sqrt{\frac{j_1}{V_1^{3/2}}} = 1340 \sqrt{\frac{30 \times 10^{-3}}{400^{3/2}}} = 2.60 \text{ db./cm.} \tag{22}$$

For a drift space 25 cm. long the gain predicted theoretically would be 65 db.

THE ELECTRON OPTICAL PROBLEM

General Requirements

According to the design presented in the preceding section an electron gun system had to be constructed to produce two beams of electrons occupying a common space and having voltages of 400 and 349 volts, respectively, and

current densities of 30 and 24.5 milliamperes per square centimetre, respectively. Furthermore, it was desired to have these voltages and currents continuously variable over as wide a range as possible so that they could be adjusted experimentally for best results. To produce either beam alone would have been relatively simple in spite of the high current densities. However, the requirement that the two beams be completely intermingled complicated the problem considerably. The possibility was investigated of producing the two beams in separate electron guns, side by side, and then mixing them by means of a suitable electrostatic deflection system. Although not impossible, a calculation of the physical dimensions involved revealed the impracticability of the scheme. The alternative method, which was used, utilized two electron gun systems placed one behind the other along the axis of the tube and having the front gun transparent to the beam from the back gun. An electrode configuration which promised to fulfil these requirements in a reasonably satisfactory manner and to provide sufficient electrical and electron-optical flexibility was developed using the rubber membrane analogue of the system.

The Rubber Membrane Analogue Method

Theory of the Analogue

Problems dealing with potential fields in two dimensions can be represented by the surface of a rubber membrane uniformly stretched over a model of the electrode configuration being studied. Positive electrodes are arranged to push down into the rubber surface from above while negative electrodes push upward beneath the membrane. The surface of the rubber provides a topographical representation of the variations in the potential field. To predict the motions of electrons in such a field small steel balls (of diameter about one eighth of an inch) can be allowed to roll over the surface. Provided the slope of the surface does not anywhere exceed approximately ten degrees and the path lengths are not long enough to make frictional losses appreciable, a reasonably accurate picture of the electron motion can be obtained. The great advantage of the method, as a means of designing an electron-optical system is the stimulus it provides to the imagination of the experimenter as he seeks to achieve his ends. The mathematical background of the analogy is concisely treated in Spangenberg's text (8) on page 75. The analogy is based, of course, on the fact that the elevation of the rubber surface and electrostatic

potential both satisfy Laplace's equation in two dimensions

$$d^2V/dx^2 + d^2V/dy^2 = 0.$$

Two fundamental limitations are placed on the accuracy of this method of design by analogy. Firstly, nothing in the analogue corresponds to space-charge which can be an important factor in devices having high current densities. Secondly, the rubber membrane analogue cannot exactly represent a potential field having rotational symmetry about an axis, -- Laplace's equation contains a term in cylindrical coordinates which is not present in the Cartesian case. Nevertheless, the method can often provide an entirely satisfactory electrode configuration for problems that are very difficult if not impossible to solve analytically.

The Apparatus Used

The apparatus used for the design of the electron-optical system is shown in Fig. 1 and Fig. 2. The rubber membrane was about three feet by five and was equipped with metal grommets around the edge so that it could be laced into the metal frame. The metal framework supported the rubber in a level position above a flat table on which the lower electrode blocks could be placed beneath the membrane. A superstructure consisting of four lengths of pipe

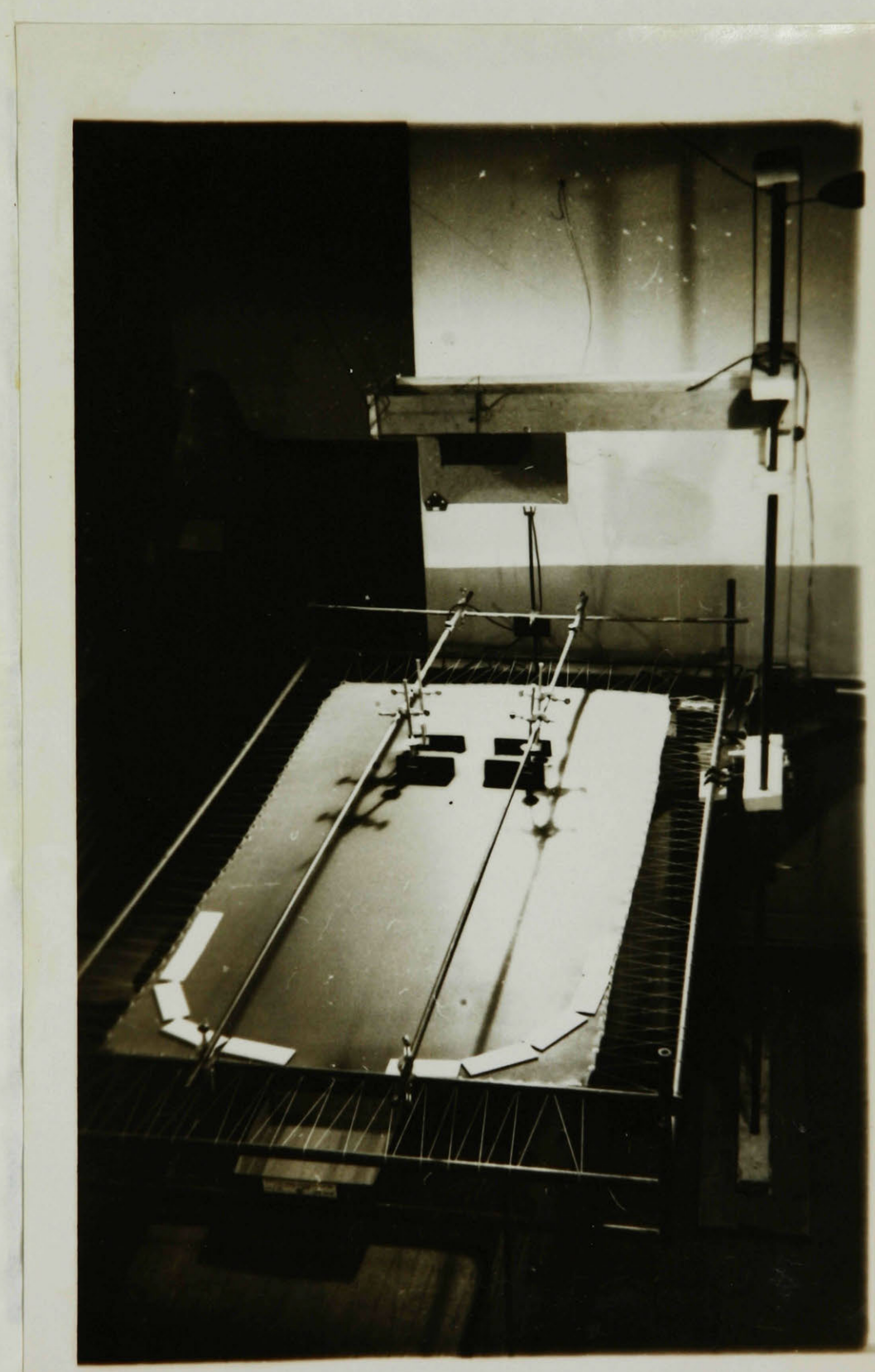

Fig. 1. Rubber Analogue Apparatus

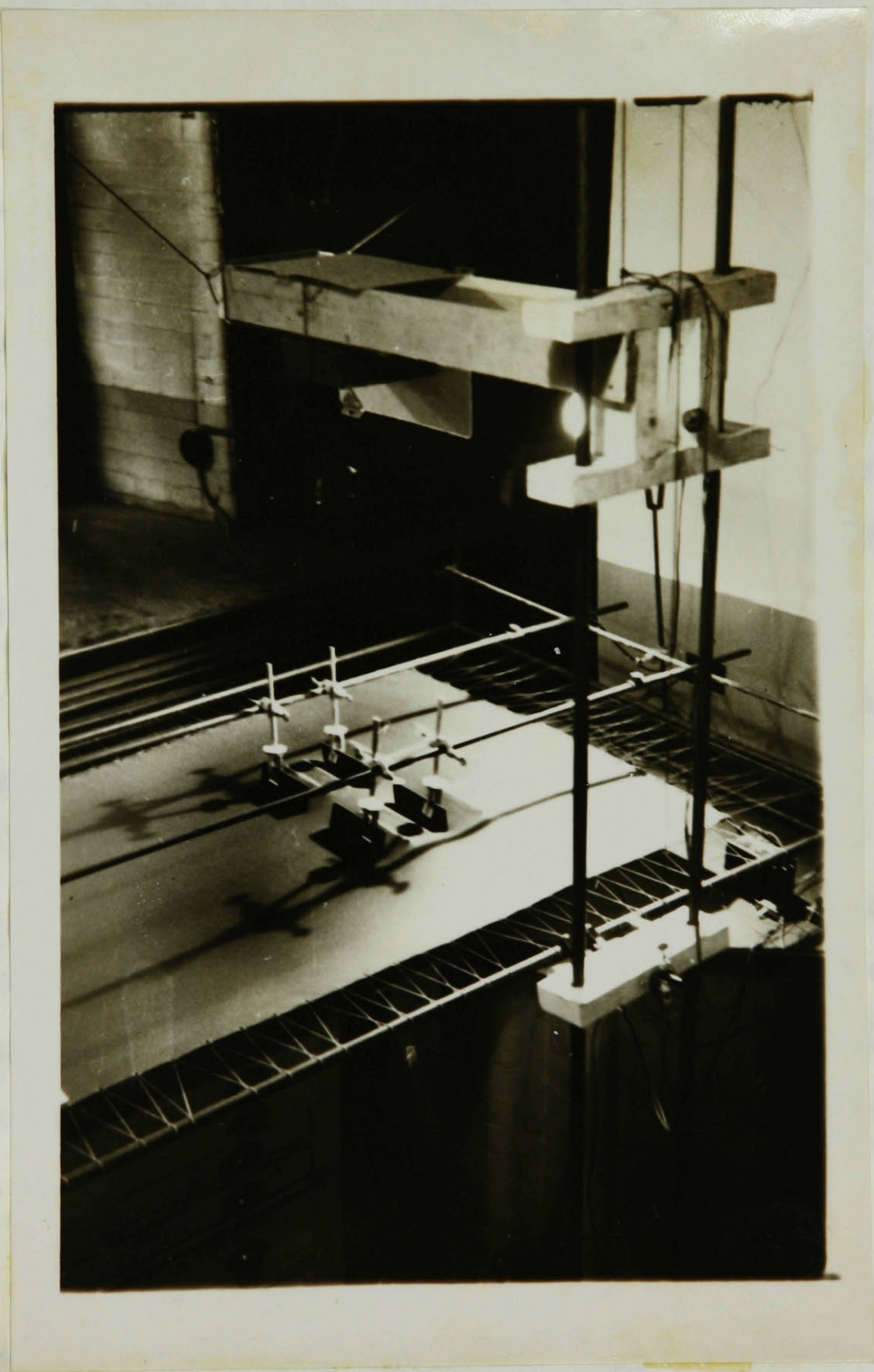

Fig. 2. Rubber Analogue Apparatus

supported clamps which held the electrodes used on top of the rubber sheet. The electrodes beneath the rubber could be raised or lowered by a suitable combination of supporting wooden blocks which were prepared in an assortment of accurate thicknesses ranging from one thirty-second to two inches; the electrodes on top could be positioned by adjustment of the clamps holding them. The electrodes themselves were made of fibre board one quarter of an inch thick. A grid of lines ruled on the rubber sheet before stretching it served to help maintain uniform tension of the membrane and facilitated the positioning of the electrodes.

It is important that the steel balls should be released with zero initial kinetic energy. This was the reason for the use of a small electromagnet from the tip of which the balls could be dropped at the opening of a switch. An improvement over this device consisted of the installation of small electromagnets directly below the rubber sheet which could hold the balls motionless until released.

In order to obtain a permanent and accurate record of the trajectories of the steel balls, a 35 mm. camera was set up on an adjustable mounting that can be seen in the first two figures overhanging the electrode

configuration on the rubber sheet. A single photoflood bulb provided the illumination. To improve the photographic contrast between the steel balls and the background the rubber was spray-painted a dull black. For the same reason the exposure was stroboscopic rather than continuous. This was accomplished by means of a rotating shutter - a motor-driven disc having a radial sector removed and passing in front of the camera lens. Consequently, the paths of the balls show in the photographs as a series of white dots against a black background.

The Design of the Electron Gun System

In addition to the specifications already outlined it was desirable that convenience of construction and simplicity of power supply requirements should be prime considerations in the choice of an electrode system. For the main focussing action it was decided to use "einzel" type lenses since such a lens is easy to build and does not alter the potential of a beam of electrons passing through it. The conventional einzed lens consists of three apertures, the two outer ones being at the same potential and the centre one at either a higher or lower potential. These lenses are described in references 8, page 349, and 9, page 98. The lens system finally adopted

was a derivation of the usual einzel lens; it consisted of four apertures - the outer two at the same potential and the inner two at a lower potential.

The various dimensions of the electrode configuration which was developed may be discussed with reference to Fig. 8 which is an outline view of a section through the axis of cylindrical symmetry. Only one of the two similar electron guns is shown. The gun system was entirely open along the axis so that a second similar electron gun, mounted directly behind, could project its beam forward. The cathode originally chosen was a circular loop, as can be seen by the two circles of crossection in Fig. 8. The cathode was surrounded by a slightly negative cylindrical electrode called the "grid cylinder", the purpose of which was to control the emission and to cause the electrons from the cathode to converge to a point on the axis marked 2 in Fig. 8. This point formed a virtual cathode which was the object for the main lens consisting of the four apertures. Dimension A was not critical except that the opening in the back of of the grid cylinder must not affect the potential at the cathode. The same criterion decided dimension P. Dimension F was identical with N so that the back surface of the grid cylinder might serve as the fourth aperture

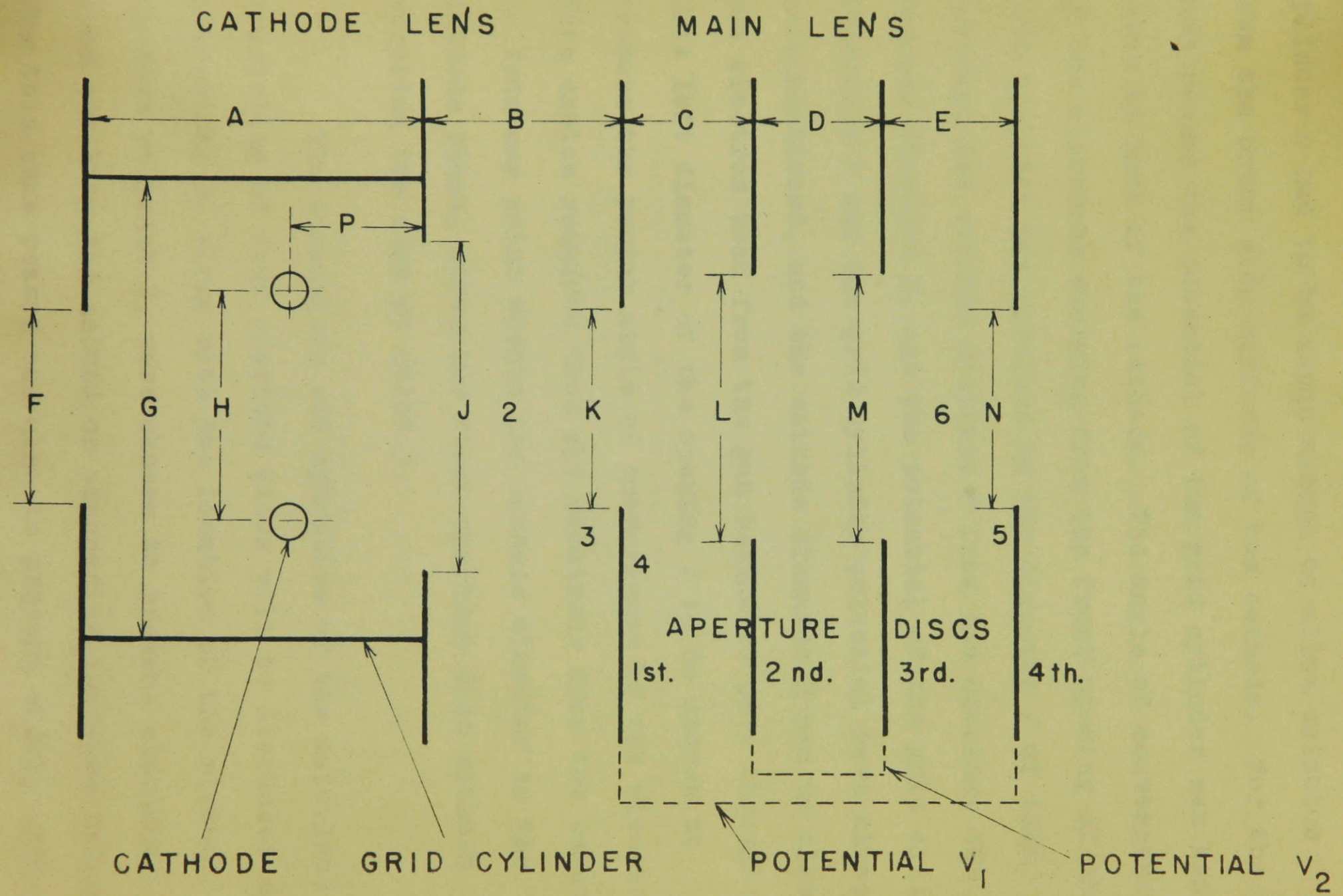

FIG. 8. FINAL GEOMETRY FOR ELECTRON GUN

disc of a preceding lens. The diameter of the grid cylinder G had to be large enough to allow emission from the outer side surfaces of the cathode. For the same reason the potential of the grid cylinder was kept close to that of the cathode. The angle of convergence of the electrons emerging from the front opening of the grid cylinder was governed by the diameter J of that opening, the cathode distance P from the opening, the cathode diameter H, and the potential of the grid cylinder; dimension P and the grid cylinder potential have already been mentioned, and the cathode diameter H had to allow the electron beam from the gun behind to pass through; this left diameter of the opening J to be chosen to produce the proper angle of convergence of the electrons. This choice required that all electrons from the cathode, or from any point within the cathode diameter in the cathode plane, enter the first aperture disc without striking the edge at point 3.

The dimensions and operation of the main lens consisting of four aperture discs will be discussed now. Dimensions B, along with the location of the virtual cathode at point 2, were chosen to prevent electrons from striking the second or succeeding aperture discs. For this same reason and also to prevent widely diverging

electrons from being turned back to point 4 by the edge of the second aperture disc, the diameters L and M of the second and third apertures were made larger than K and N, the diameters of the first and fourth apertures. The spacings C, D and E between the discs were determined so that electrons would not strike the fourth disc at point 5 and so that a moderate change of potential V_2 could produce a suitable variation of the focal length of the main lens. By adjusting the potential V_2 of the two central aperture discs the point at which the electrons crossed the axis could be varied from point 6 to 7 and on out to infinity (a divergent beam).

The relative dimensions of the electron gun system are listed in Table I. The symbols referred to are those of Fig. 8.

The advantages of the four aperture einzel lens over the conventional three aperture type are that fewer electrons strike the electrodes, the focal length can be varied over wider limits, and all electrons cross the axis more nearly at the same point (less spherical abberation).

In the stroboscopic photographs of Figs. 3 to 7 inclusive the various parts of the electrode system can

TABLE I

Relative Dimensions of the Electron Gun System as Determined on the Rubber Model

Symbol	AJ	B	CDE	FKN	G	H	LM
Size	10	6	4	6	14	7	8

The scale used in construction was one unit equals one millimetre.

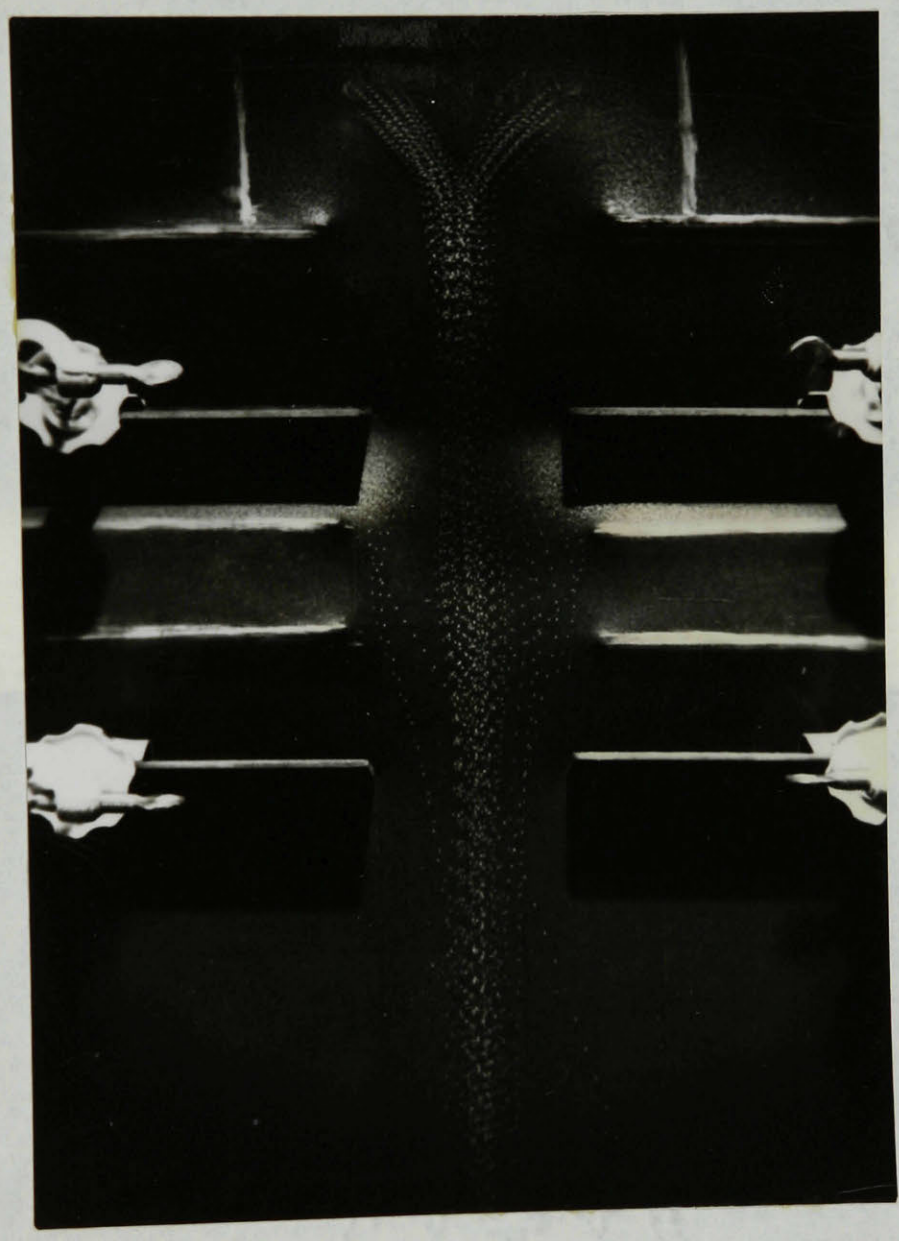

Fig. 3. General Focussing Action

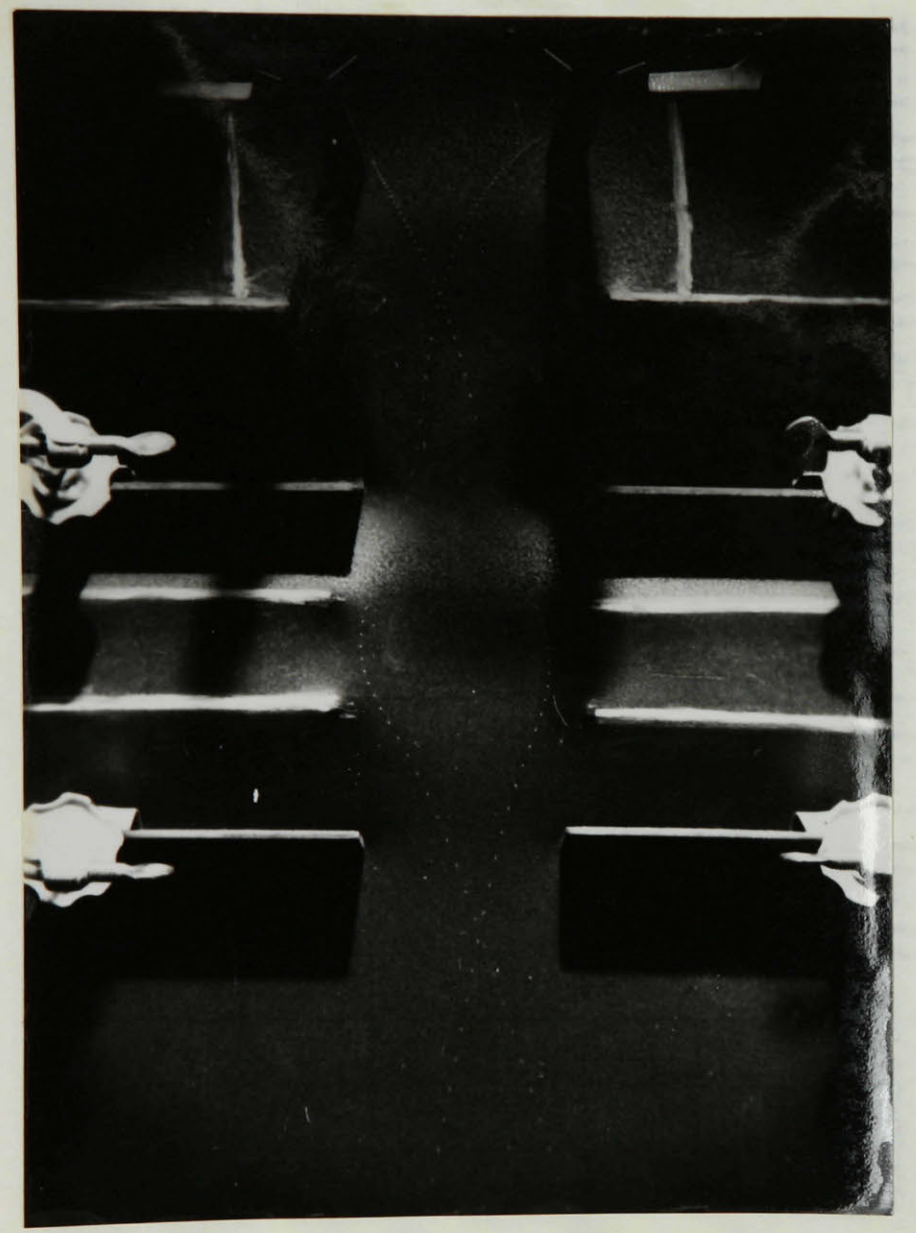

Fig. 4. Short Convergence

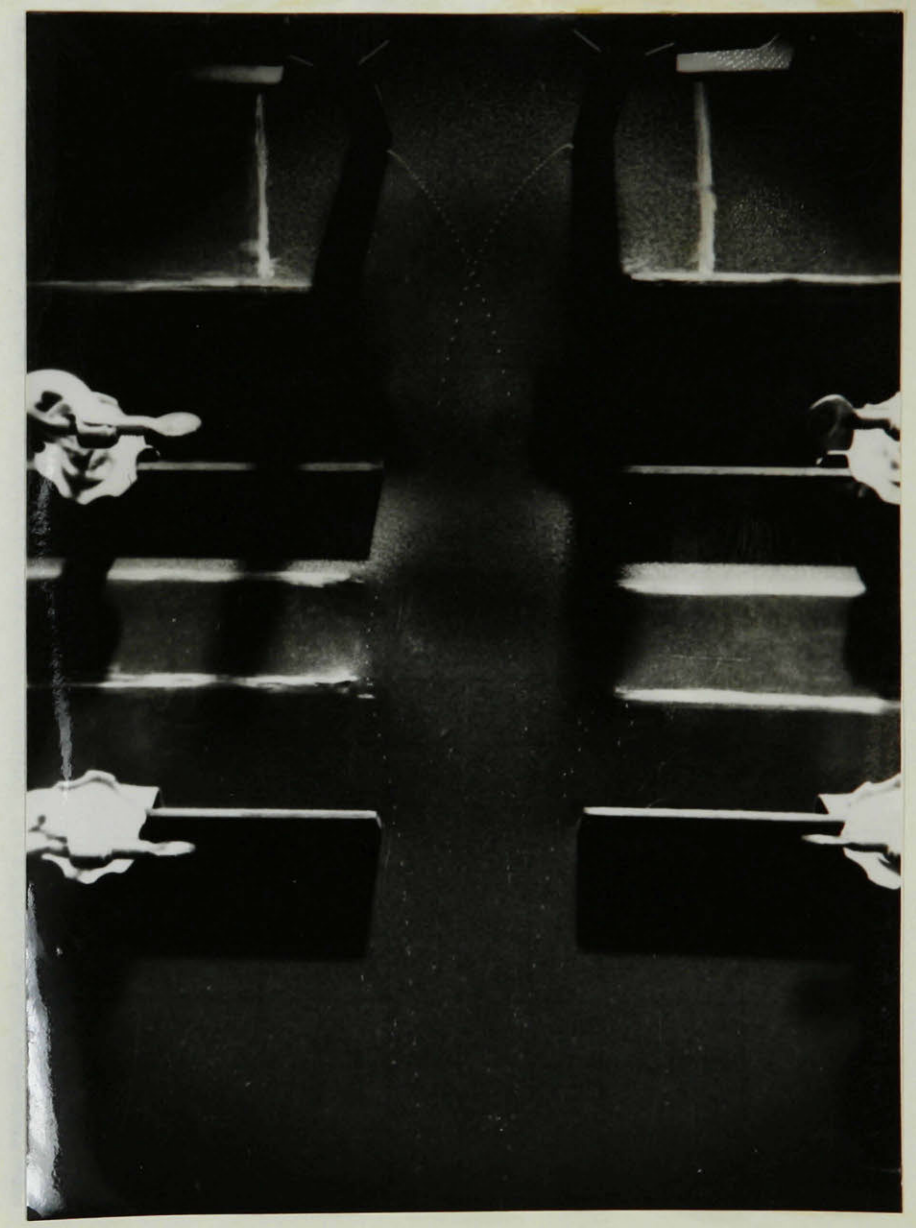

Fig. 5. Long Convergence

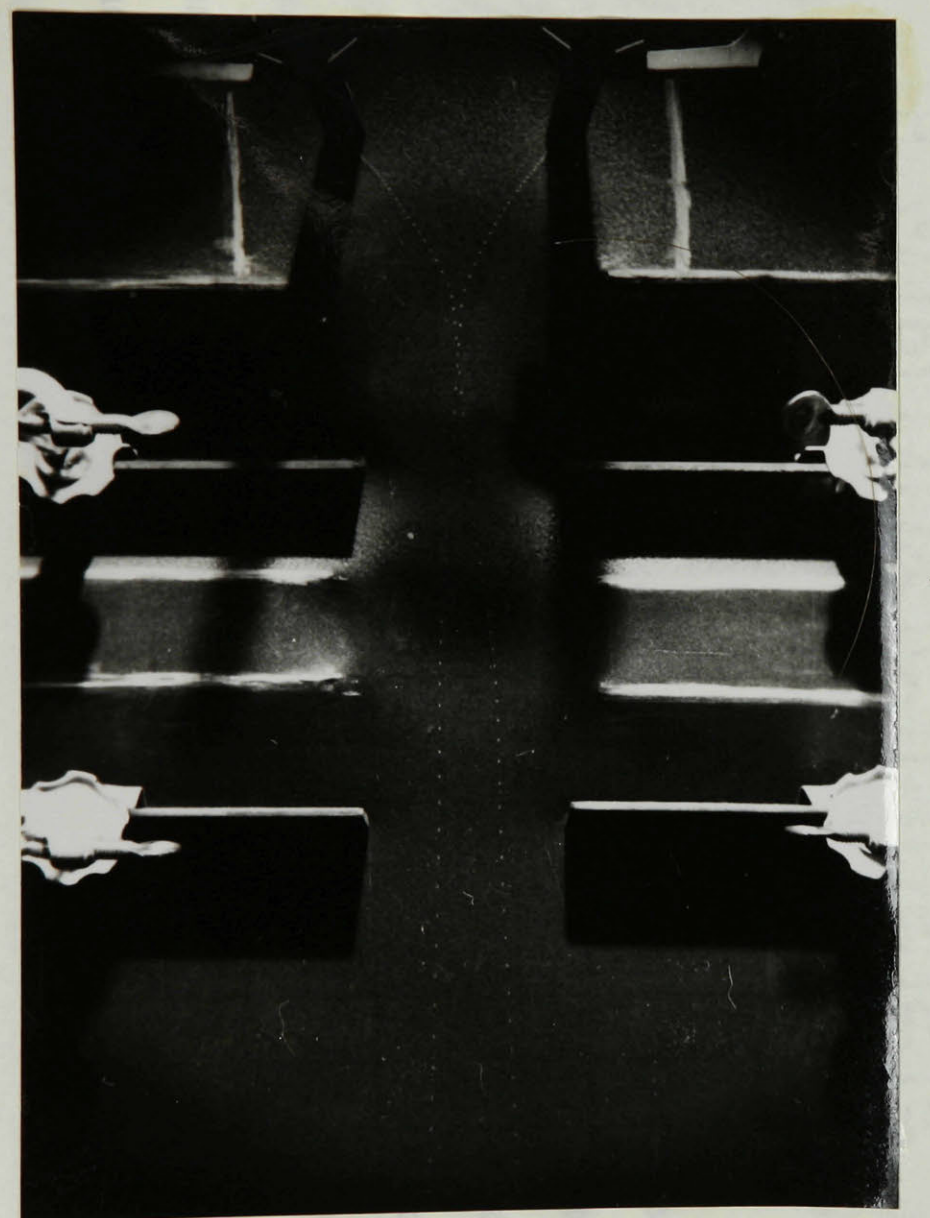

Fig. 6. Divergence

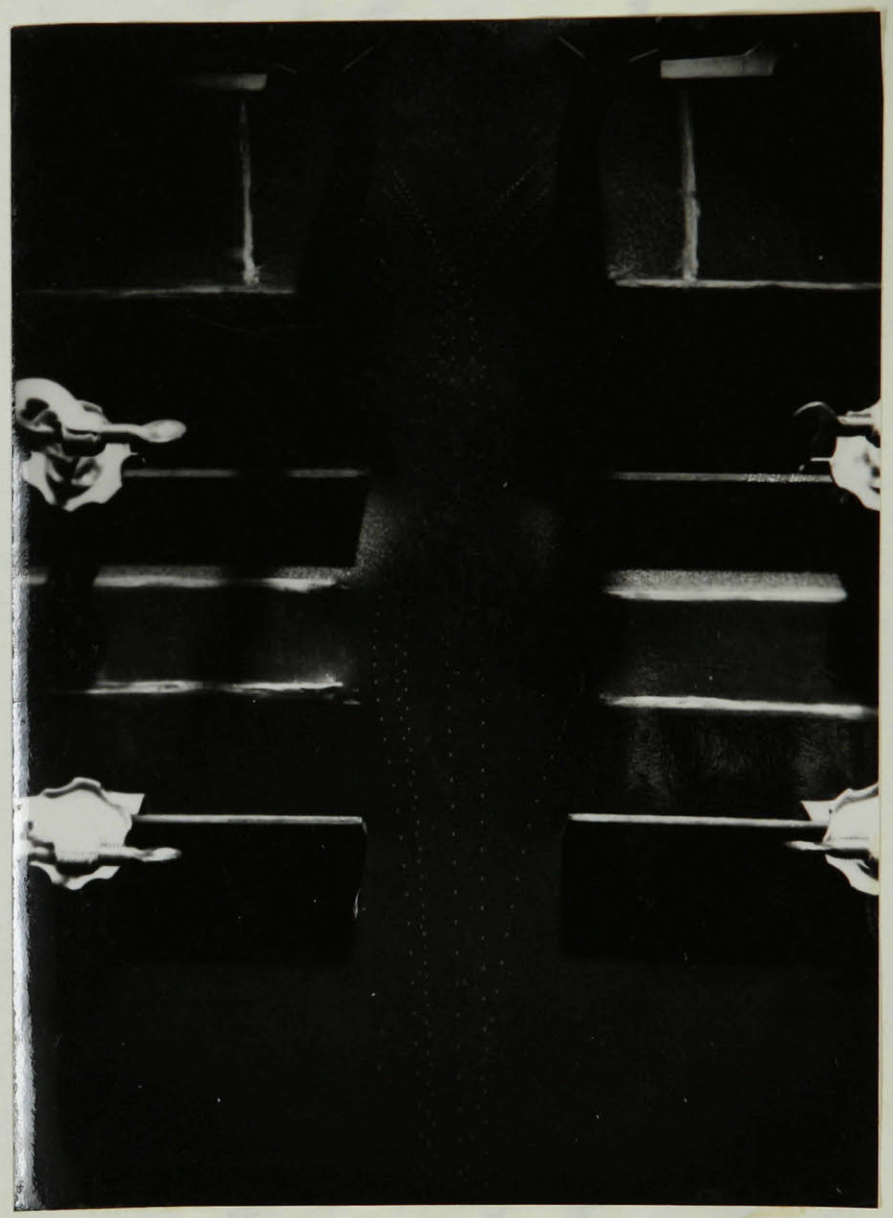

Fig. 7. Beam Formation

be seen. The cathode represented by round vertical rods can be seen near the top of the pictures. Surrounding the cathode was the grid cylinder only the forward half of which is visible. Being at a negative potential it was placed below the membrane and its position indicated by chalk lines on the rubber surface. The four aperture discs of the main lens can be seen, - the first and fourth were positive and pressed down from above while the second and third were relatively more negative and were, therefore, beneath the rubber. Two electromagnets were located beneath the rubber at the cathode positions.

Fig. 3 is a general view of the focussing action in which a large number of balls were released at one time. The formation of a beam is clearly displayed. A more accurate study of the focussing action is afforded in Figs. 4, 5 and 6 in which only two steel balls were used. The location of the virtual cathode where the two balls first cross the axis, as well as the focal point in front of the main lens can be seen. The potential V_2 of the second and third aperture discs was made progressively less negative in going from Figs. 4 to 5 to 6. Fig. 4 shows a short convergent action such as was used for the back electron gun so that its beam could penetrate the front gun structure and be formed into a parallel beam by the main lens of the front gun. Fig. 5

shows a longer convergence and Fig. 6 a complete divergence. A potential ratio for the main lens somewhere between that used for Fig. 5 and Fig. 6 was used to obtain the photograph Fig. 7, which was approximately the manner in which the front electron gun operated in the final electron-optical system.

In a report such as this it is obviously necessary to omit description of the very numerous trial and error adjustments and observations that preceded the final choice of electrode arrangement. Accordingly, an attempt has been made to summarize the process of selection of values of the many variables involved.

Structural Details of the Electron Gun System

The various pieces which made up the electron gun system are shown in Figs. 9 to 17 inclusive and Fig. 18 is a photograph of the completely assembled structure before it was installed in the tube. Precision of alignment was assured by machining the brass parts on a lathe and by using accurately sawn glass spacers to separate the electrodes. The electrodes (discs as shown in Fig. 9) were mounted on three glass rods, separated by glass spacers and held rigid by a mechanical super-structure consisting of three threaded brass rods bolted

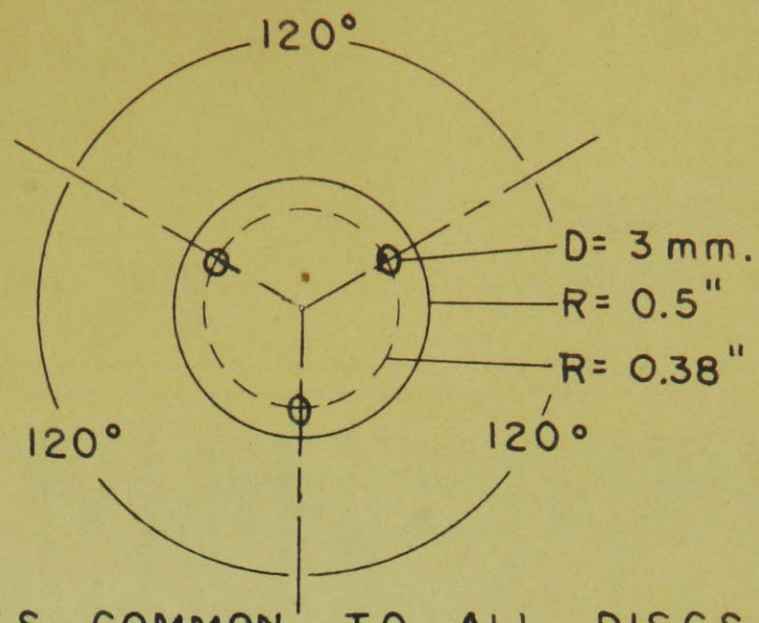

FIG. 9. DETAILS COMMON TO ALL DISCS (X 1)

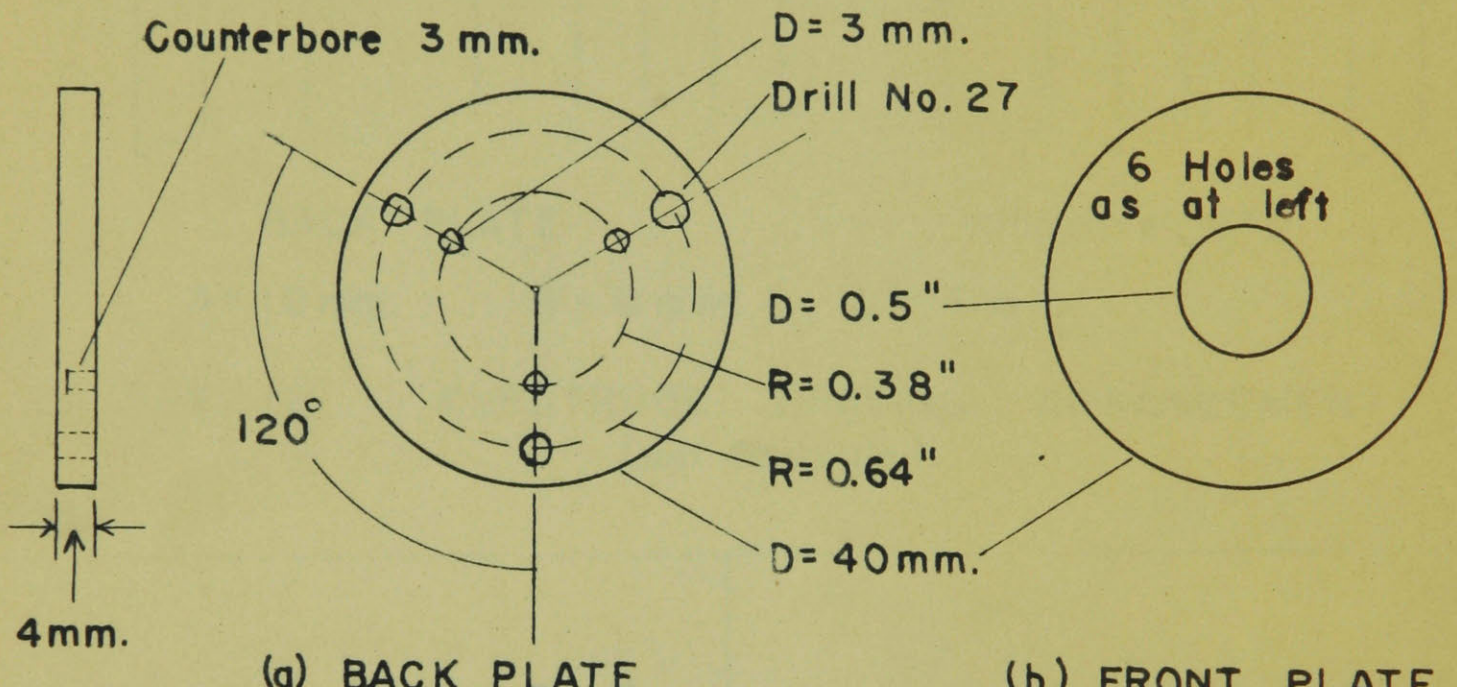

(a) BACK PLATE (b) FRONT PLATE

FIG. 10. (X 1)

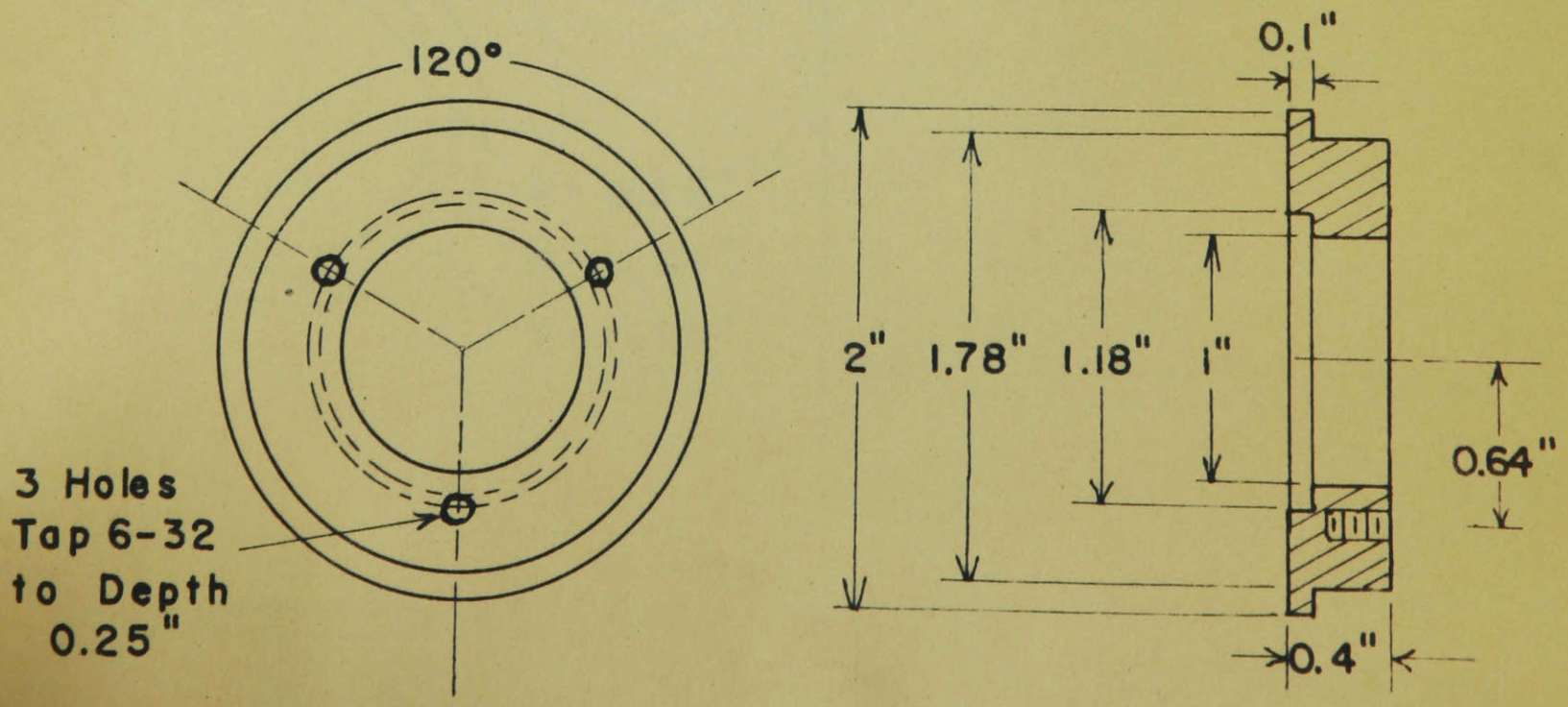

FIG. 11. END PLATE (X 1)

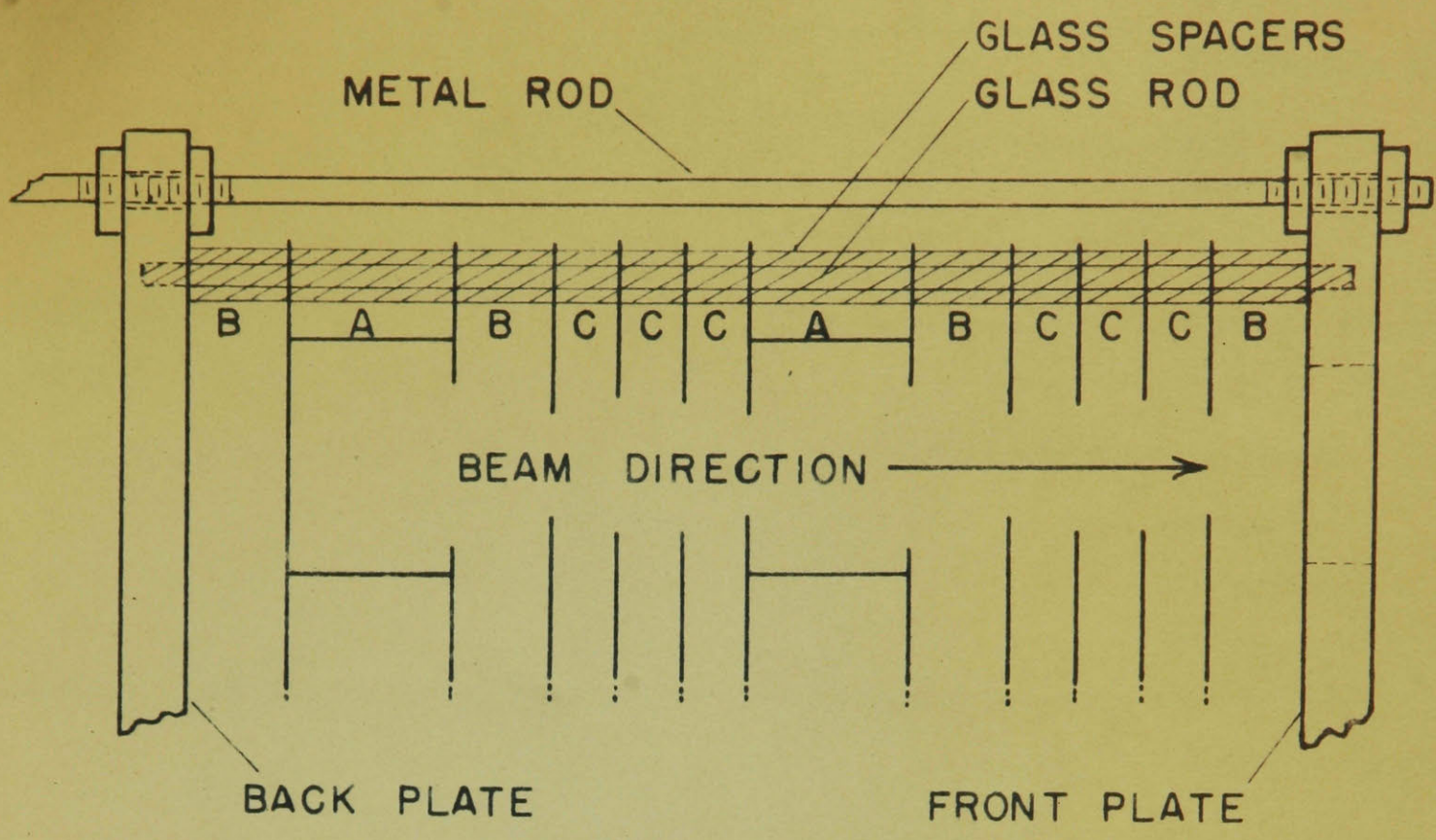

FIG. 12. ELECTRODE SPACING ARRANGEMENT
(not to scale)

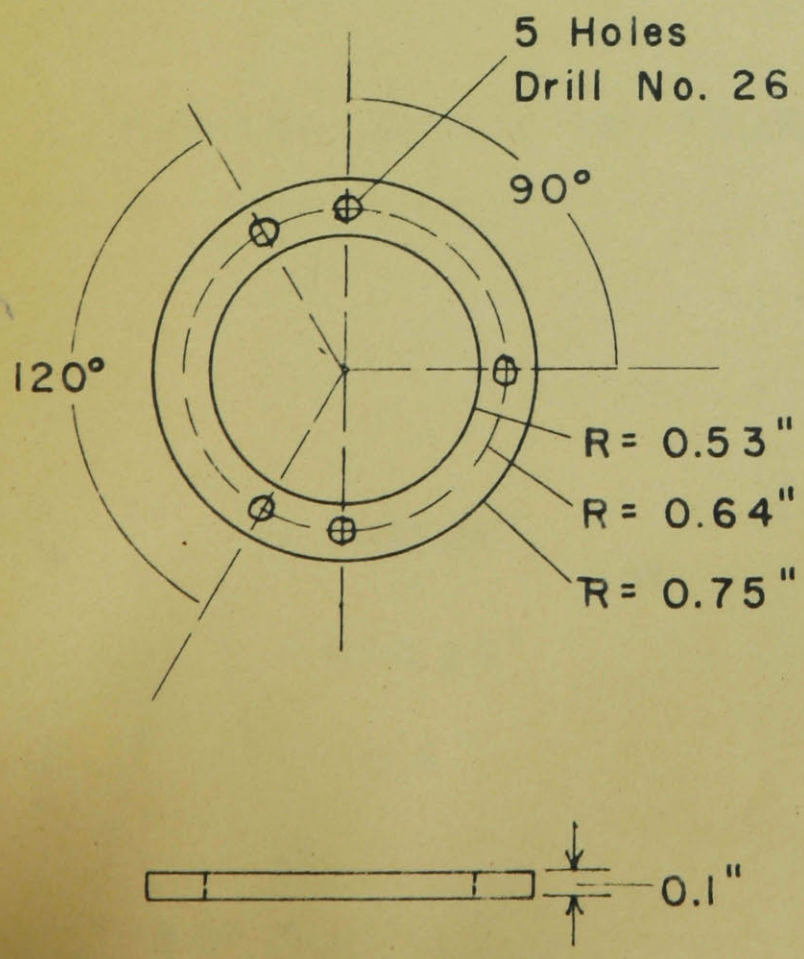

FIG. 13. FILAMENT MOUNTING RING (X1)

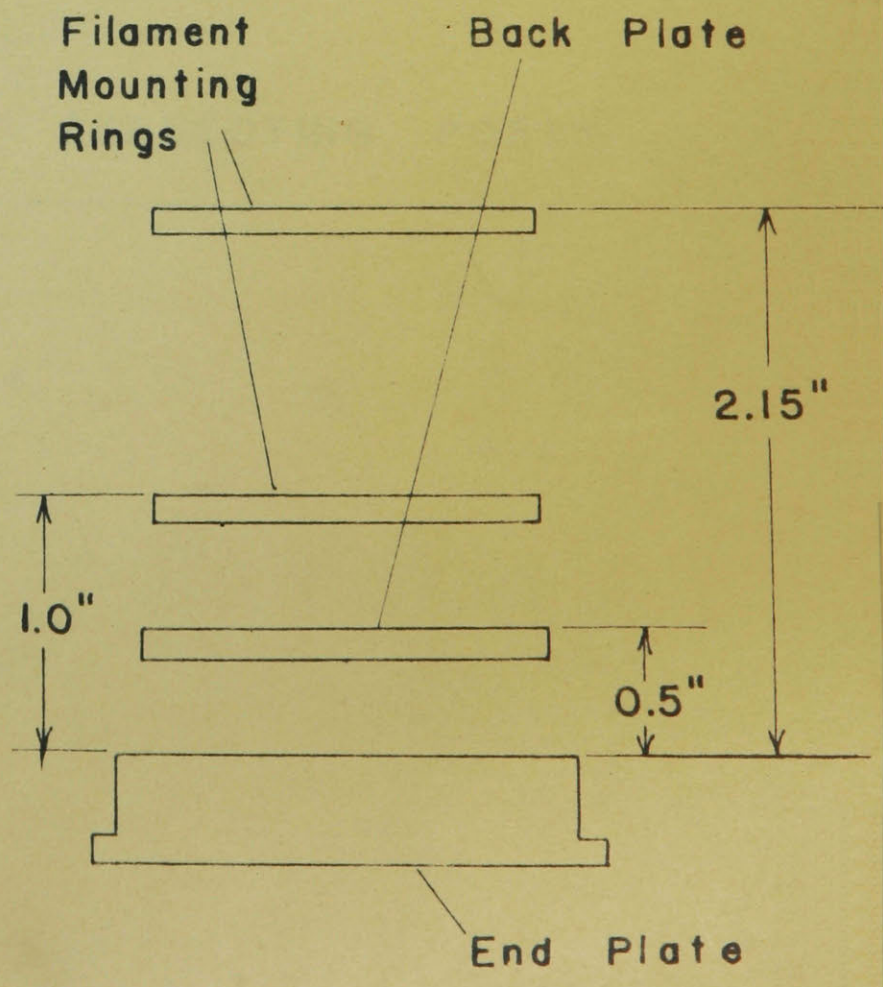

FIG. 14. POSITION OF FILAMENT MOUNTING RINGS (X1)

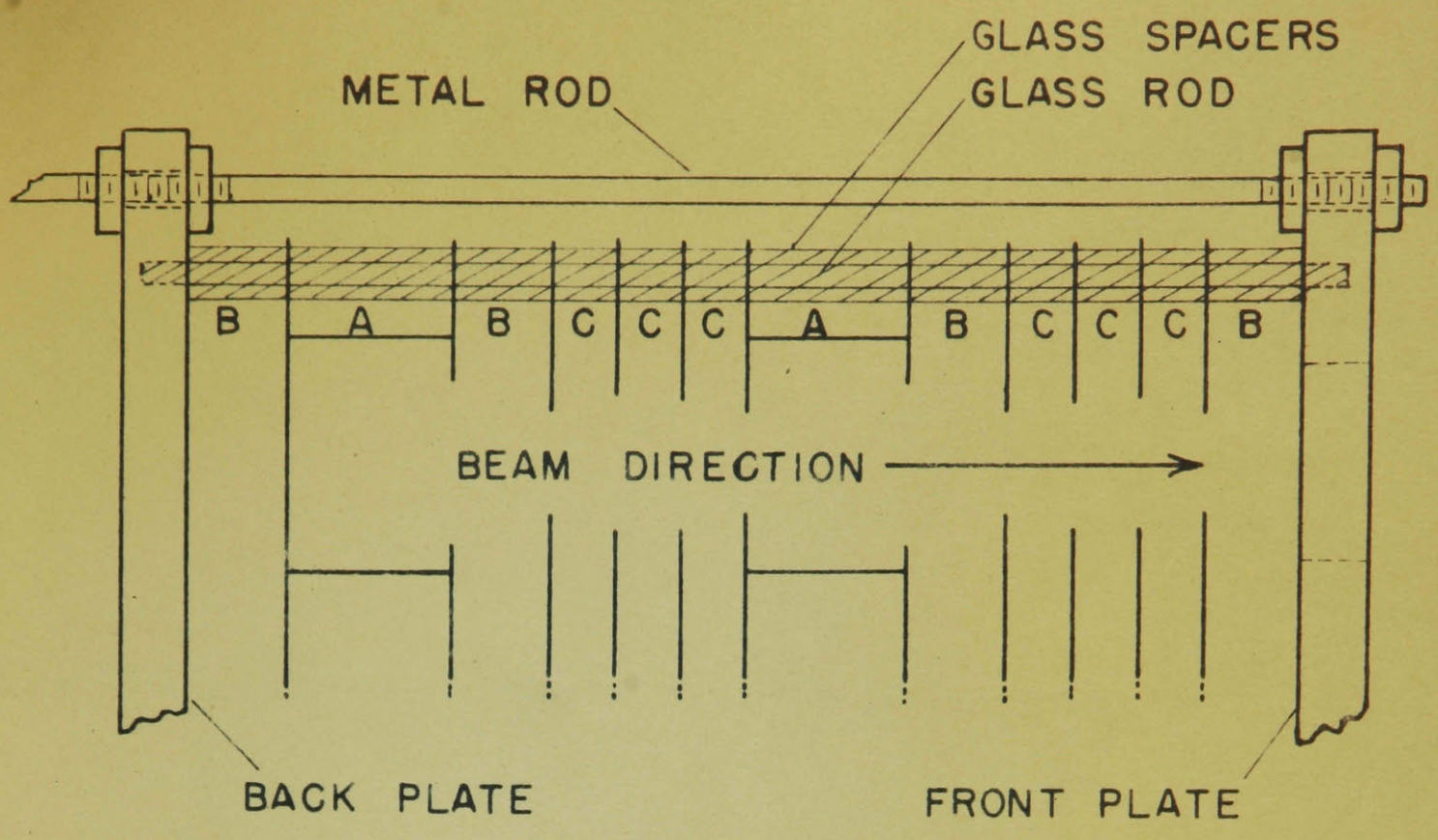

A = 10 mm. B = 6 mm. C = 4 mm.

FIG. 12. ELECTRODE SPACING ARRANGEMENT
(not to scale)

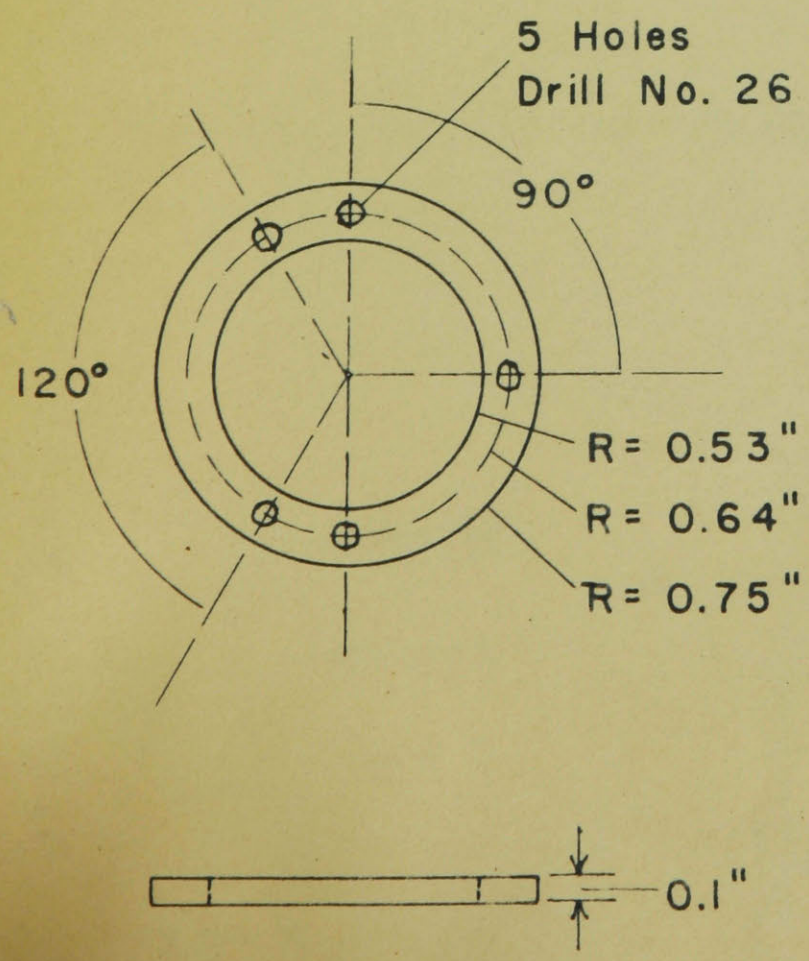

FIG. 13. FILAMENT MOUNTING RING (X1)

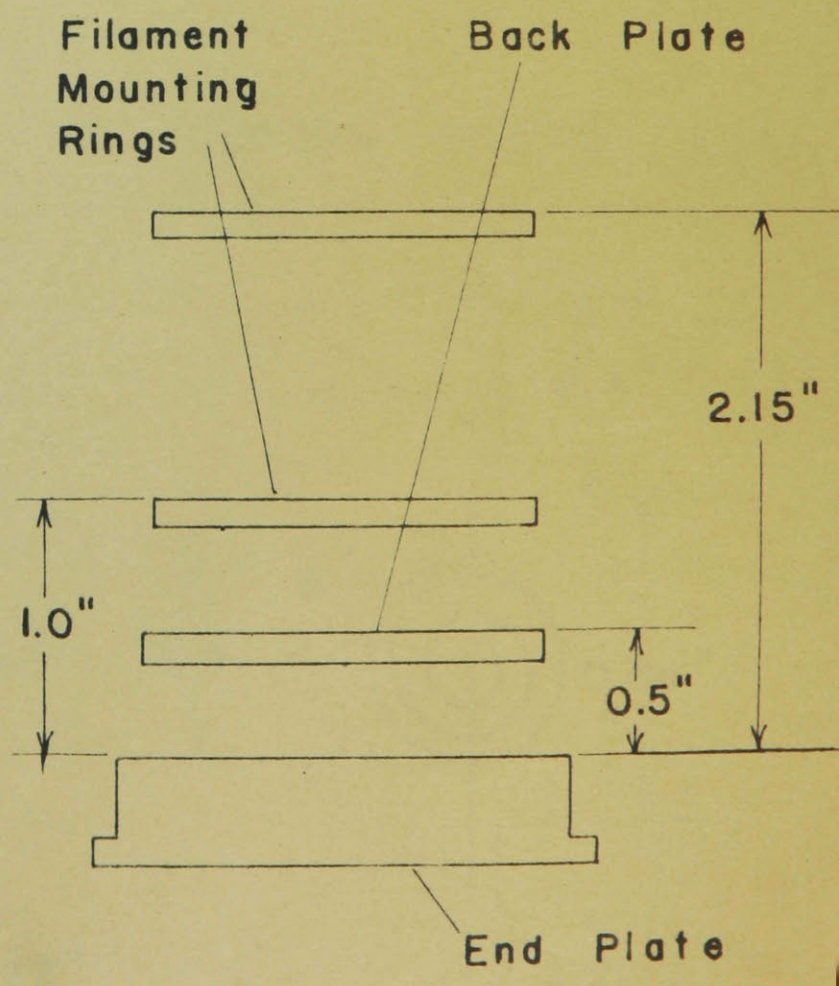

FIG. 14. POSITION OF FILAMENT MOUNTING RINGS (X1)

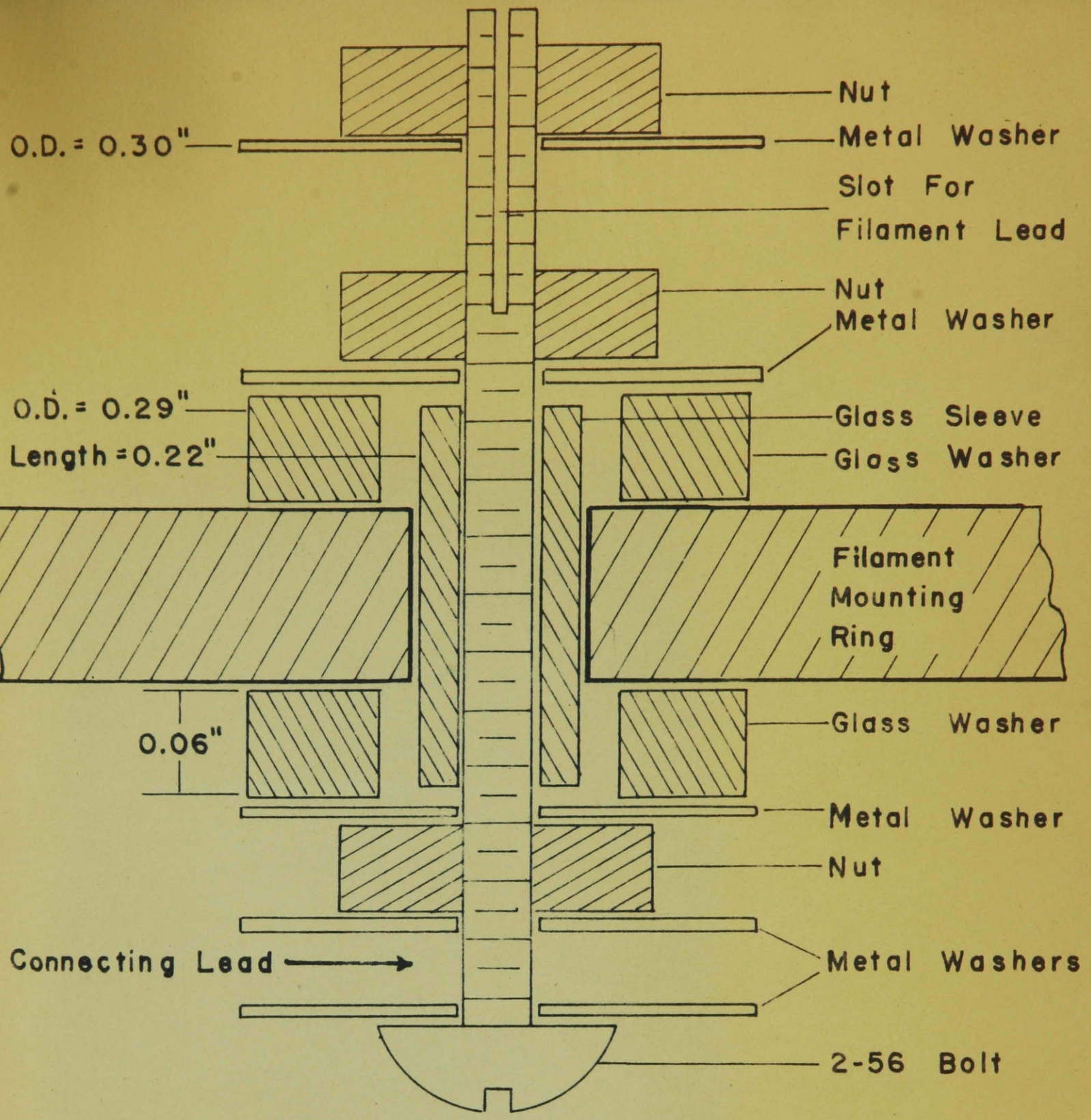

FIG. 15. DETAIL OF FILAMENT CONNECTING POSTS (X 10)

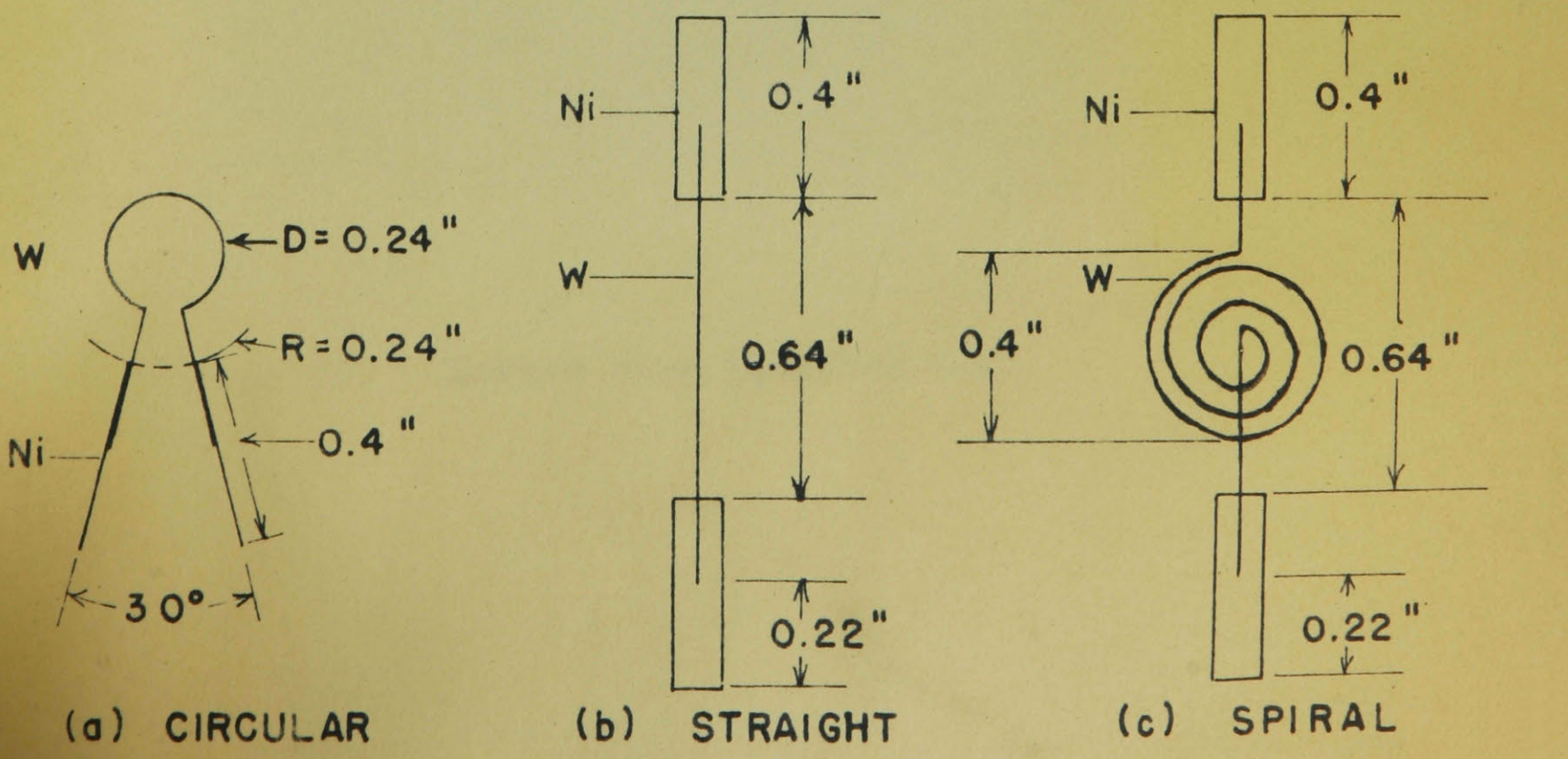

FIG. 16. FILAMENT FORMS (X 2)

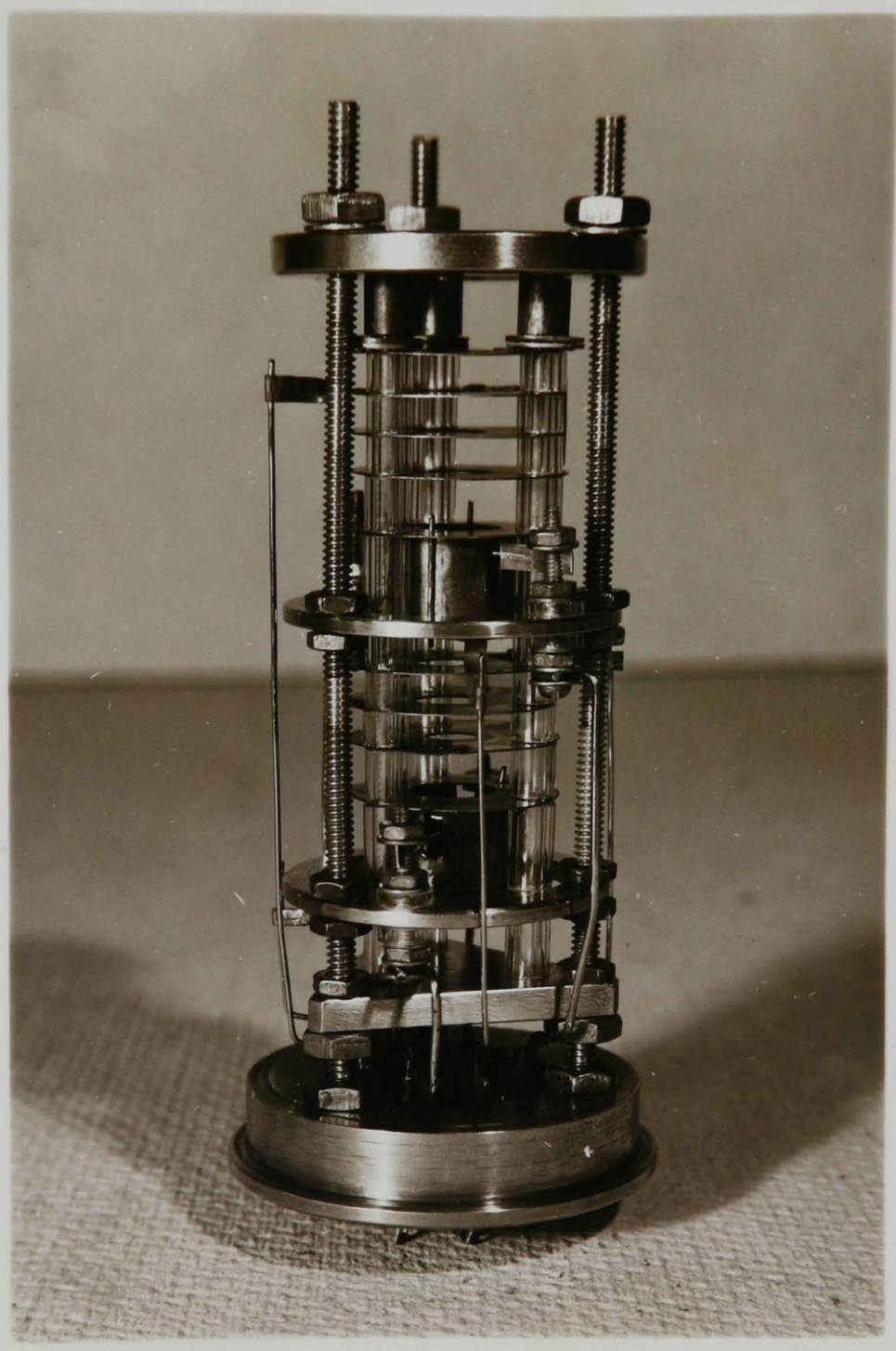

Fig. 18. Double Beam Electron Gun

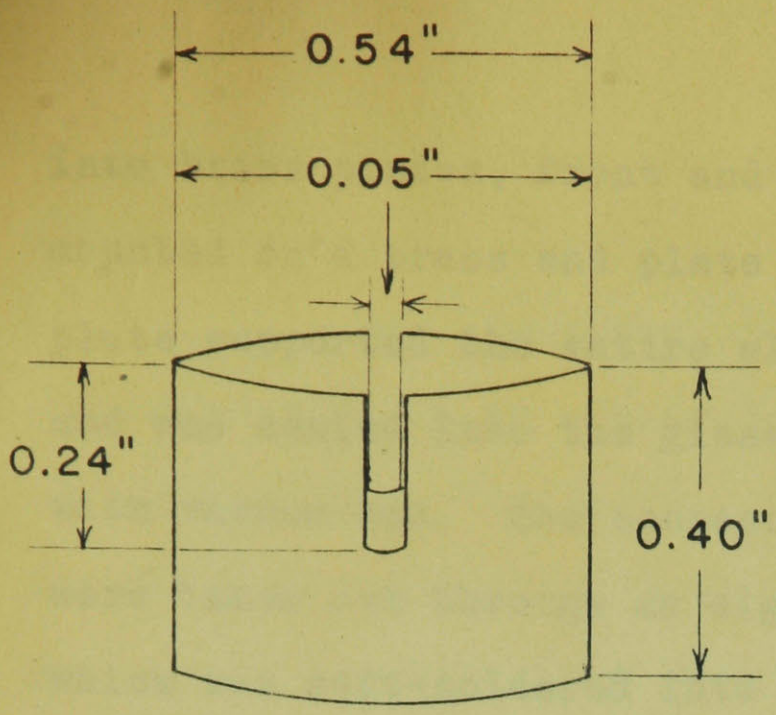

FIG. 17a. GRID CYLINDER (X3)

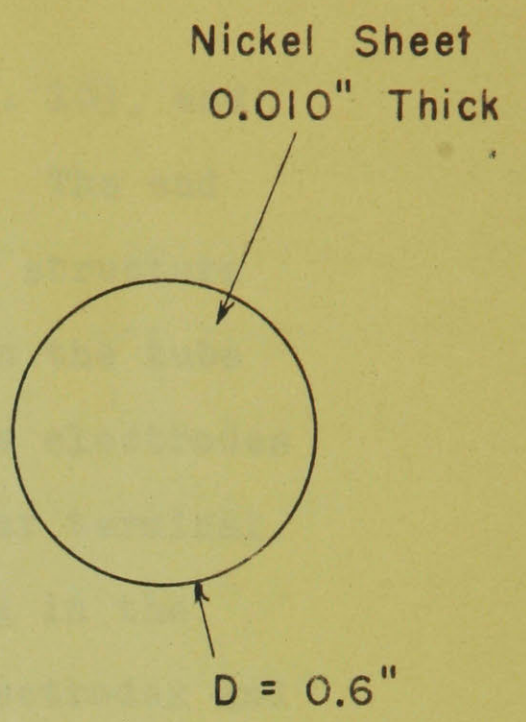

FIG. 17b. COLLECTOR ELECTRODE (X2)

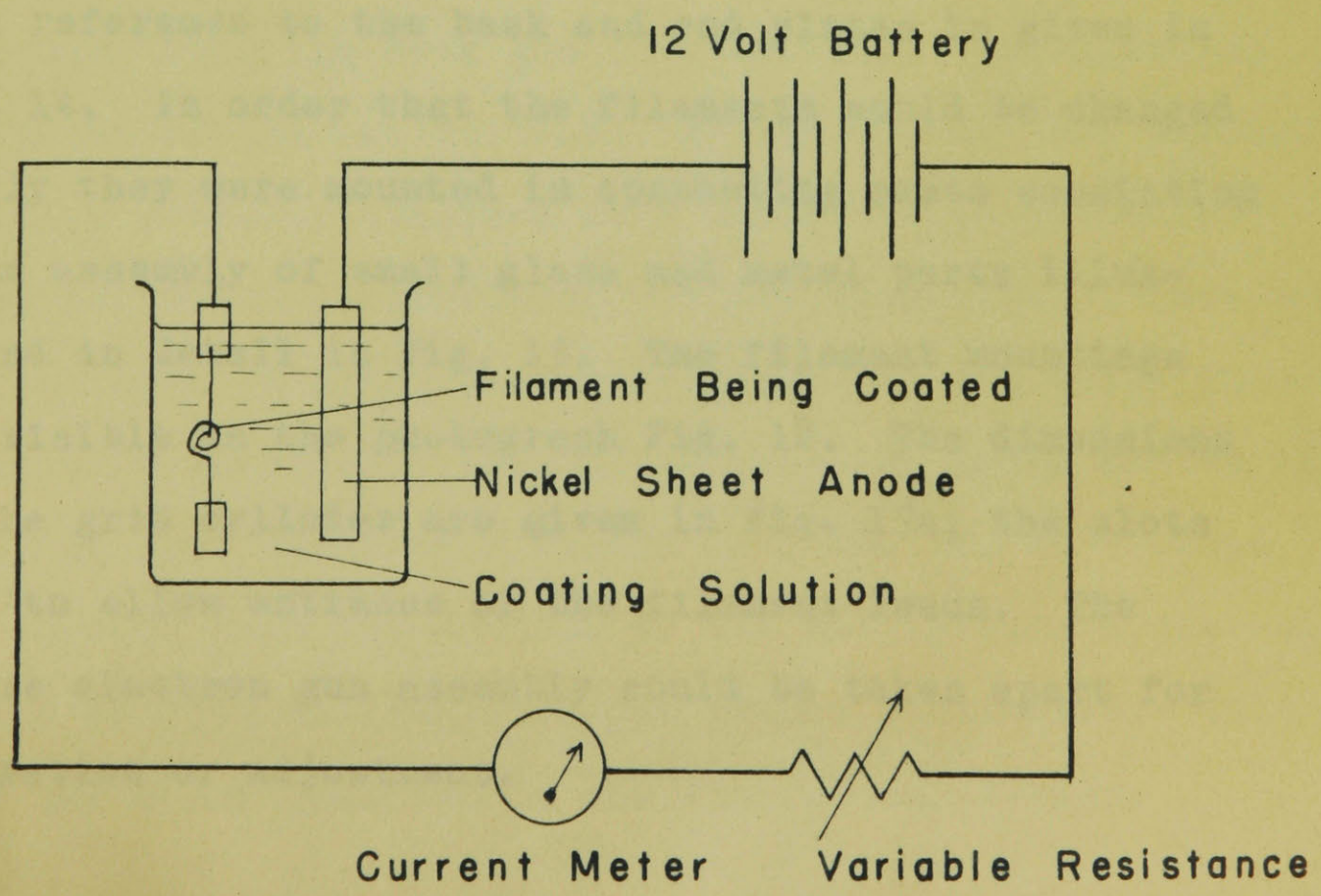

FIG. 19. CIRCUIT FOR THORIA COATING PROCESS

into brass plates, front and back, (Fig. 10), and mounted on a brass end plate (Fig. 11). The end plate supported the entire electron gun structure and was sealed into the glass housing on the tube with vacuum wax. The connections to the electrodes were taken out through an eight pin kovar terminal which was soft-soldered into the opening in the brass end plate. The spacing of the electrodes and the arrangement of the supporting structure is displayed in Fig. 12. The filaments were mounted on two rings that slid over the three threaded brass rods and could be locked into position at any level. One of these rings is shown in Fig. 13 while their position with reference to the back and end plates is given in Fig. 14. In order that the filaments could be changed easily they were mounted in connecting posts consisting of an assembly of small glass and metal parts illustrated in detail in Fig. 15. The filament mountings are visible in the photograph Fig. 18. The dimensions of the grid cylinder are given in Fig. 17a; the slots were to allow entrance of the filament leads. The entire electron gun assembly could be taken apart for alteration or adjustment.

Three different shapes of filamentary cathodes were tried experimentally. The original circular design of Fig. 16 a was abandoned when it was found to give an asymmetrical beam of electrons due to the lower temperature of the part near the leads. For the front gun a straight filament gave adequate emission and did not impede the passage of the beam from behind. In order to obtain sufficient current from the back gun a spiral filament (Fig. 16c) was used.

In accordance with the design previously worked out from theory, the back gun could be operated at 51 volts and the front gun at 349 volts. This would provide an electron beam from the front gun at a velocity of 349 volts and a beam from the back gun at a velocity corresponding to the sum of the two voltages, or 400 volts. The current densities actually obtained were difficult to estimate. The rubber model photographs, for instance Fig. 3, show the beam confined to approximately the central one third portion of the exit aperture. This final aperture had a radius of 3 mm., so that assuming a radius of 1 mm. for an average beam current from one cathode of 0.8 ma., yields a current density of 29.5 milliamperes per square centimetre. This is of the order demanded by the theoretical design.

The Process of Thoria Coating the Cathodes

The filamentary cathodes were made of tungsten wire 0.010 in. in diameter and were coated to a depth of approximately 0.005 in. with thorium oxide by a process of cataphoresis. The thoria coating improved the emission over that of pure tungsten by a large factor. Although the type of barium-strontium oxide coating conventionally used for cathodes in vacuum tubes has a still higher emission, it is damaged by air after it has been activated. Since the tube had to be assembled and disassembled many times, the use of thoria coatings which can be repeatedly reactivated was dictated.

The process of applying a thoria coating by cataphoresis was described by Hanley (10). The simple circuit used is shown in Fig. 19. The solution is made up in the proportions of 5 grams of thoria, 0.075 grams of thorium nitrate, thoroughly mixed in 100 millilitres of 95% ethyl alcohol. The object to be coated is cleaned in carbon tetrachloride, in water and finally in ethyl alcohol, and is connected as the cathode in the circuit. The current and time required depend on the area of the object to be coated; in this case a current of 0.2 ma. flowed for five minutes. Fig. 20 is a photograph of the apparatus used. It shows a filament held in a clamp

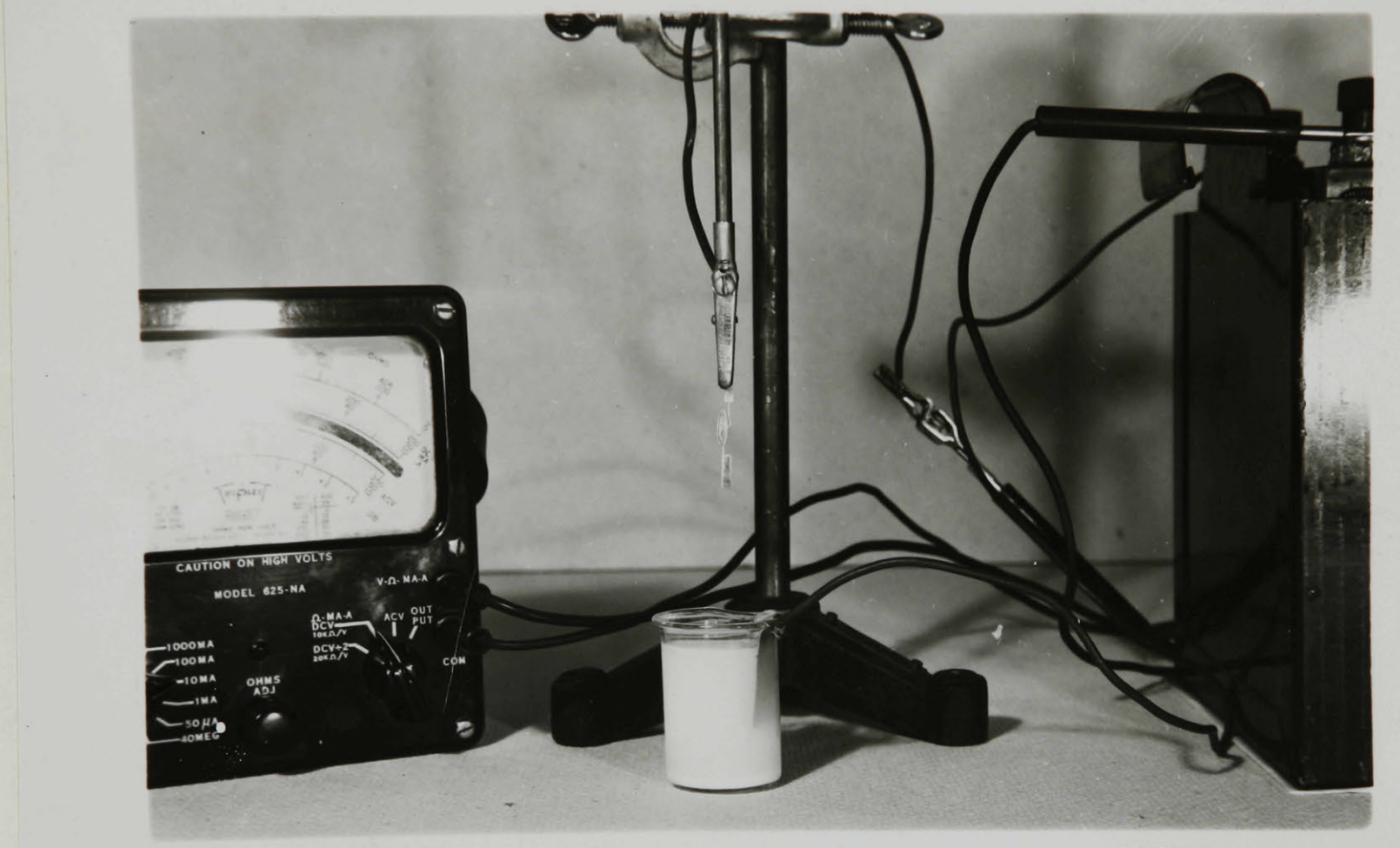

Fig. 20. Apparatus For Thoria Coating Process

above a small beaker containing the thoria solution. On the left is the current meter and on the right a 12 volt storage battery.

The activation process is similar to that commonly employed with thoriated tungsten cathodes (page 39, reference 8). For one or two minutes the cathode is heated to 2800°K. during which time some of the thorium oxide is reduced to metallic thorium. The second stage requires from 20 to 30 minutes at a temperature of 2200°K. during which time the electron emission will build up from a very low value by a factor of about 1000. Finally, the emission current ceases to increase and the cathode is ready for operation at 1900°K.

THE CONSTRUCTION OF THE TUBE

The tube was built in a demountable form so that changes could be made as the experimental work progressed. Vacuum seals were made with piceine wax and the tube was continuously pumped while in operation. The essential parts were a glass housing for the electron gun system, suitably machined mountings for the resonant cavities, a non-magnetic drift tube between the cavities, and a final electrode to collect the electron streams. The details of construction

and the materials used are given in Fig. 21. The metal to metal seals were soldered while the glass to metal junctions were made vacuum tight with wax. The metal parts were turned on a lathe and the glass pieces cut with a glass saw. The tube could be slipped in or out of the two coils which served to confine the electron beams magnetically, and the resonant cavities could be installed or removed as desired.

The arrangement for mounting each of the resonant cavities consisted of metal flanges accurately matching the cavity's dimensions and separated by a glass cylinder which was sealed in with vacuum wax. A pair of grids made of fine knitted tungsten mesh completed the electromagnetic circuit of each cavity. The only successful technique discovered for mounting these grids was to stretch the mesh over the brass and to hammer the fine tungsten wires into the brass with a piece of steel. This type of mounting proved permanent and generally satisfactory.

The inner diameter of the drift tube was chosen such that it would behave as a circular waveguide beyond cutoff at a wavelength of 10 centimetres. The formula (11) applicable to this problem is

$$d = (kb)\, Y/\pi \quad \text{cm.} \qquad (23)$$

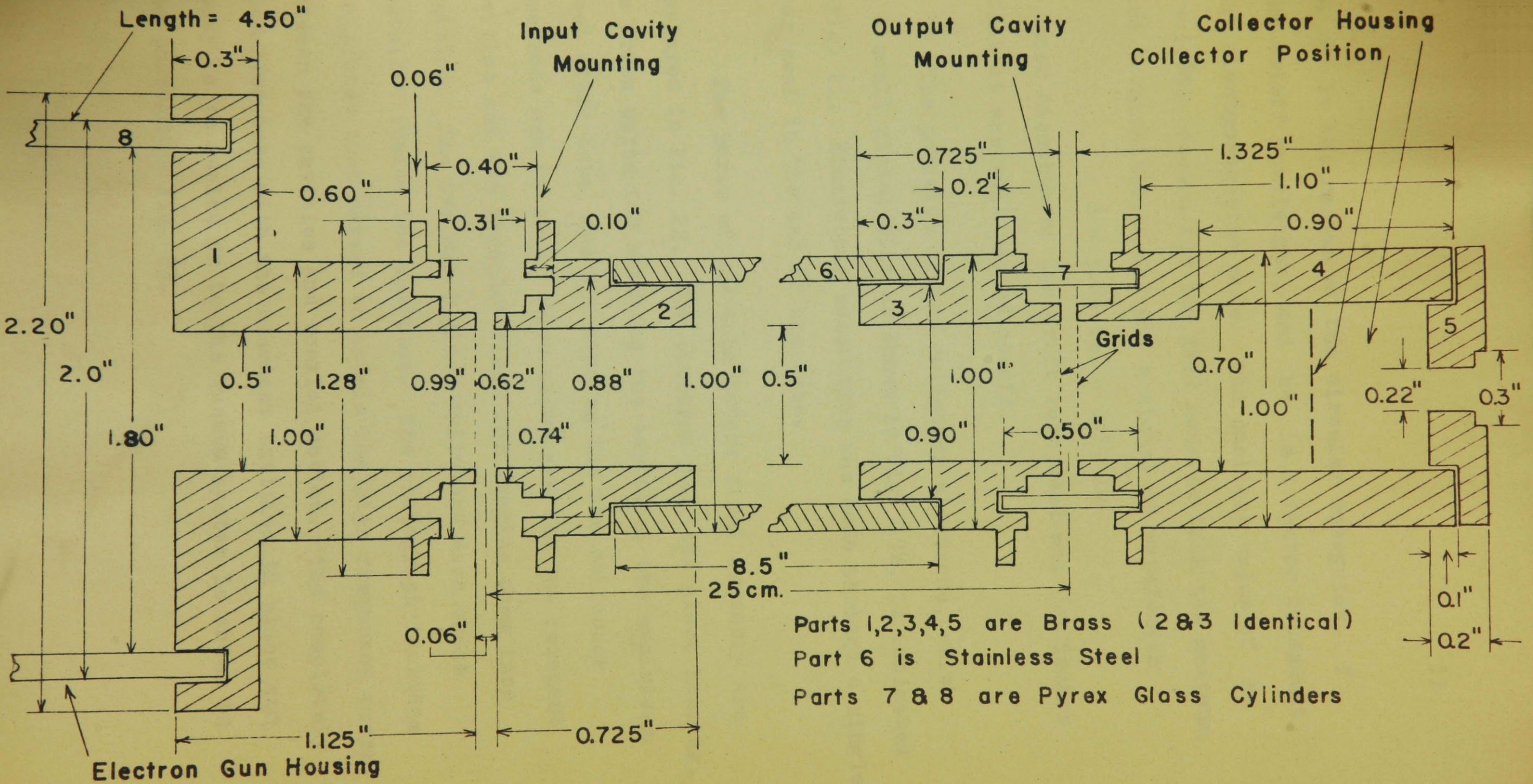

FIG. 21. STRUCTURAL DETAILS OF TUBE DESIGN (X2)

where d is the radius of the circular waveguide, Y is the cutoff wavelength, and kb is a factor dependent on the electromagnetic mode. The smallest value of kb (kb = 1.84) occurs for the TE11 mode so that the maximum radius permissible to cut off a signal of wavelength

$$d = 5.86 \text{ cm.} = 2.30 \text{ in.}$$

The inner diameter of the drift tube used was 0.9 inches so that it was well beyond cutoff.

The position of the collector electrode, which was a small nickel disc as shown in Fig. 17b, is indicated in Fig. 21. Electrical connection was made through a single kovar seal in the end of the tube.

The parts of the tube before final assembly are displayed in Fig. 22. The electron gun, its glass housing, the brass parts for mounting the cavities, the stainless steel drift tube, and the housing for the collector electrode can be seen. Also shown are the two resonant cavities and the threaded rings for locking them into position. The two small glass cylinders were those installed inside the cavities. The photograph includes two probes that served to couple the high frequency energy between the cavities and coaxial cables. The completely assembled tube with the resonant cavities in place and ready to be sealed on to the vacuum system is shown in the photograph Fig. 23.

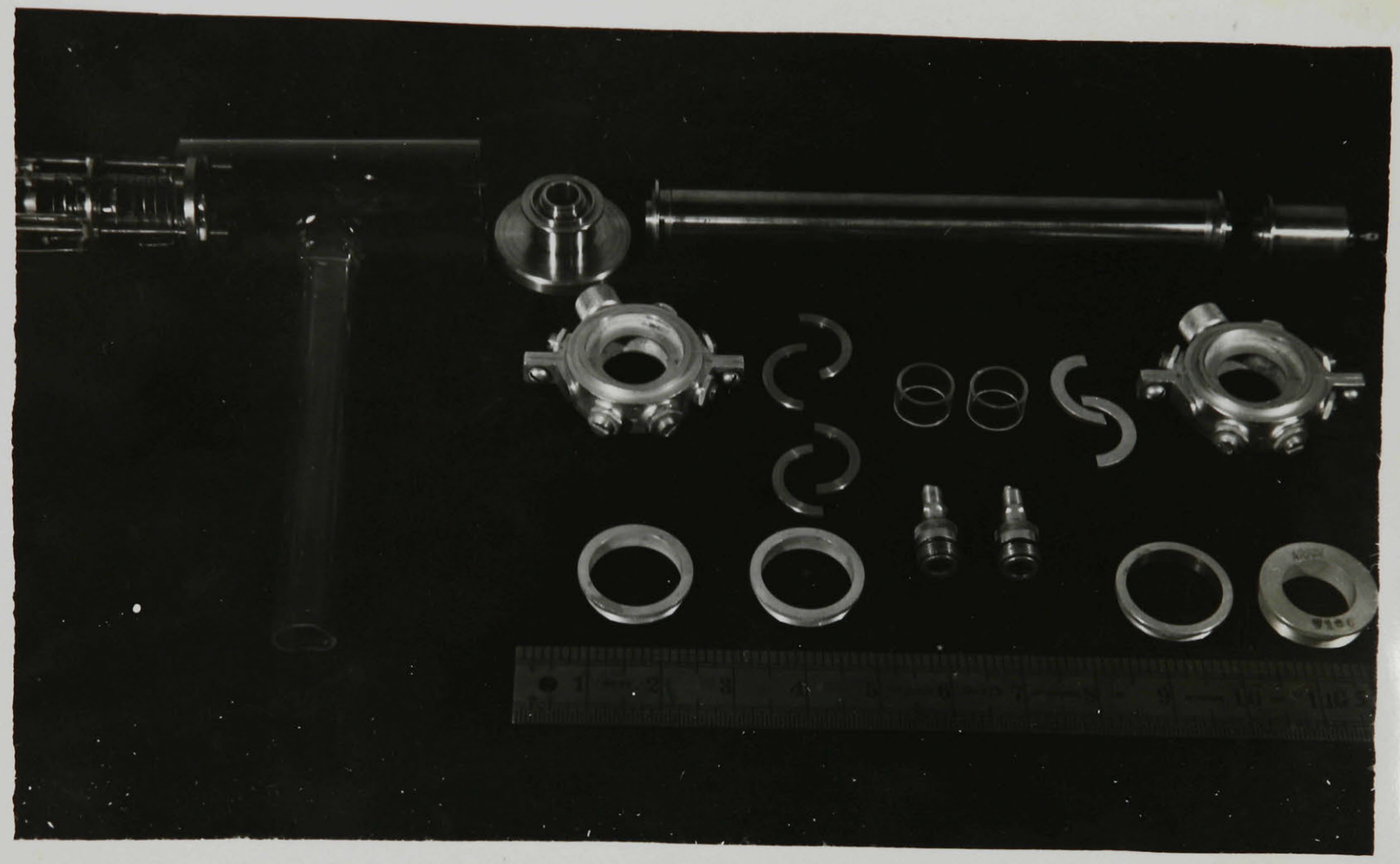

Fig. 22. Tube Parts Before Assembly

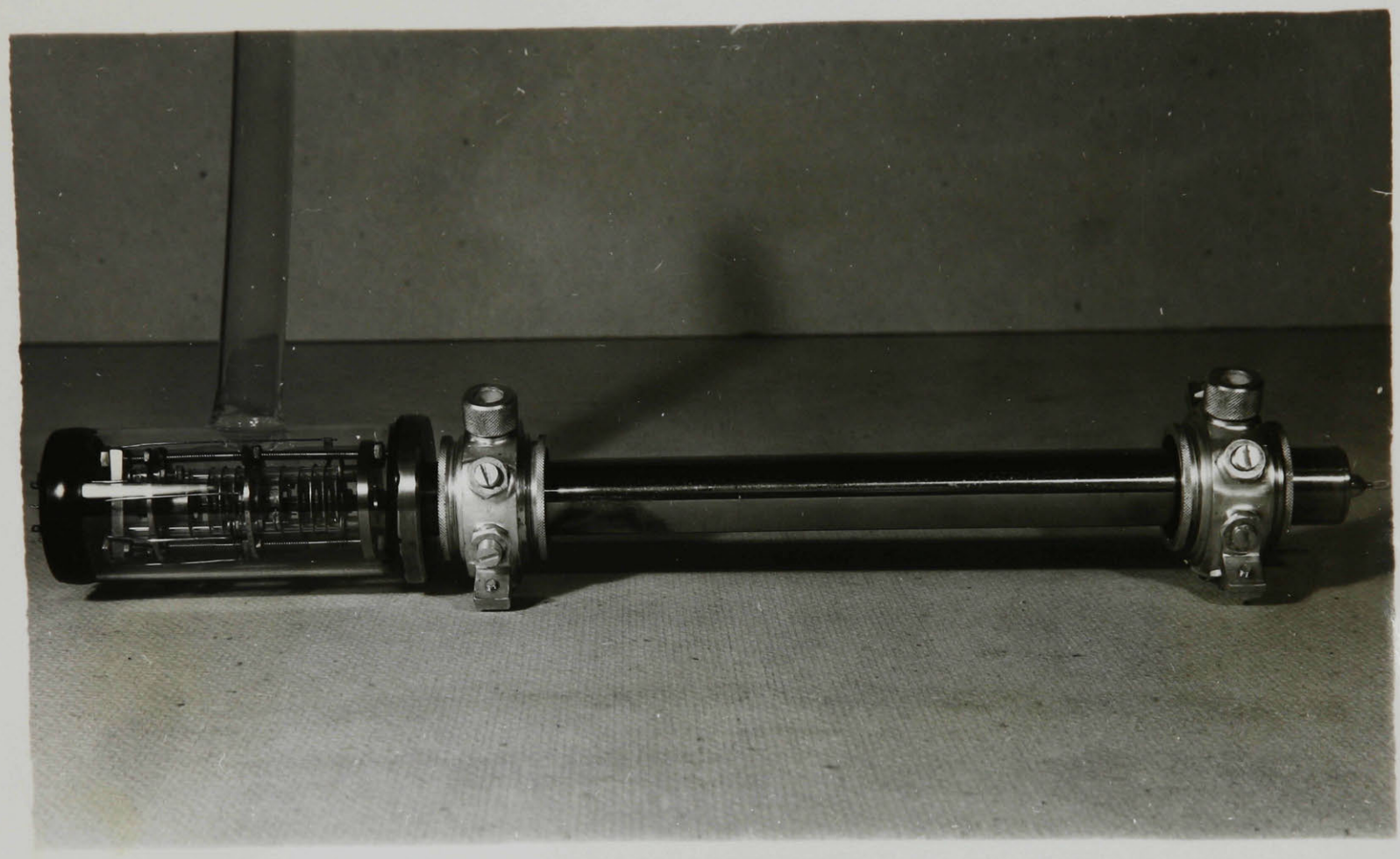

Fig. 23. The Completed Double-Stream Amplifier Tube

EXPERIMENTAL MEASUREMENTS

General Apparatus

A high quality vacuum system capable of producing an ultimate vacuum of 10^{-7} mm. of mercury was assembled. It is shown in schematic form in Fig. 24. Directly below the experimental tube was the ion gauge which measured the high vacuum pressure. A glass three-stage fractionating diffusion pump was separated from the mechanical pump by a drying tube. The backing pressure at the exhaust of the diffusion pump was measured on a thermocouple gauge.

The electrical circuitry is shown in the diagram of Fig. 25. It consisted of a network of potentiometers that served to divide a 600 volt regulated supply into the voltages required by the tube, and a number of meters to measure the important voltages and currents. The meters and their purposes are listed in Table II. The ground of the electrical circuit was connected to the metal body of the tube. The filaments were supplied with alternating voltage from individual variacs connected to the standard 110 volt supply. The current in the electron streams was measured on meter M9. In operation, this current was adjusted to a maximum by careful orientation of the magnetic focussing coils. The 45 volt battery in series with the collector prevented electrons being scattered

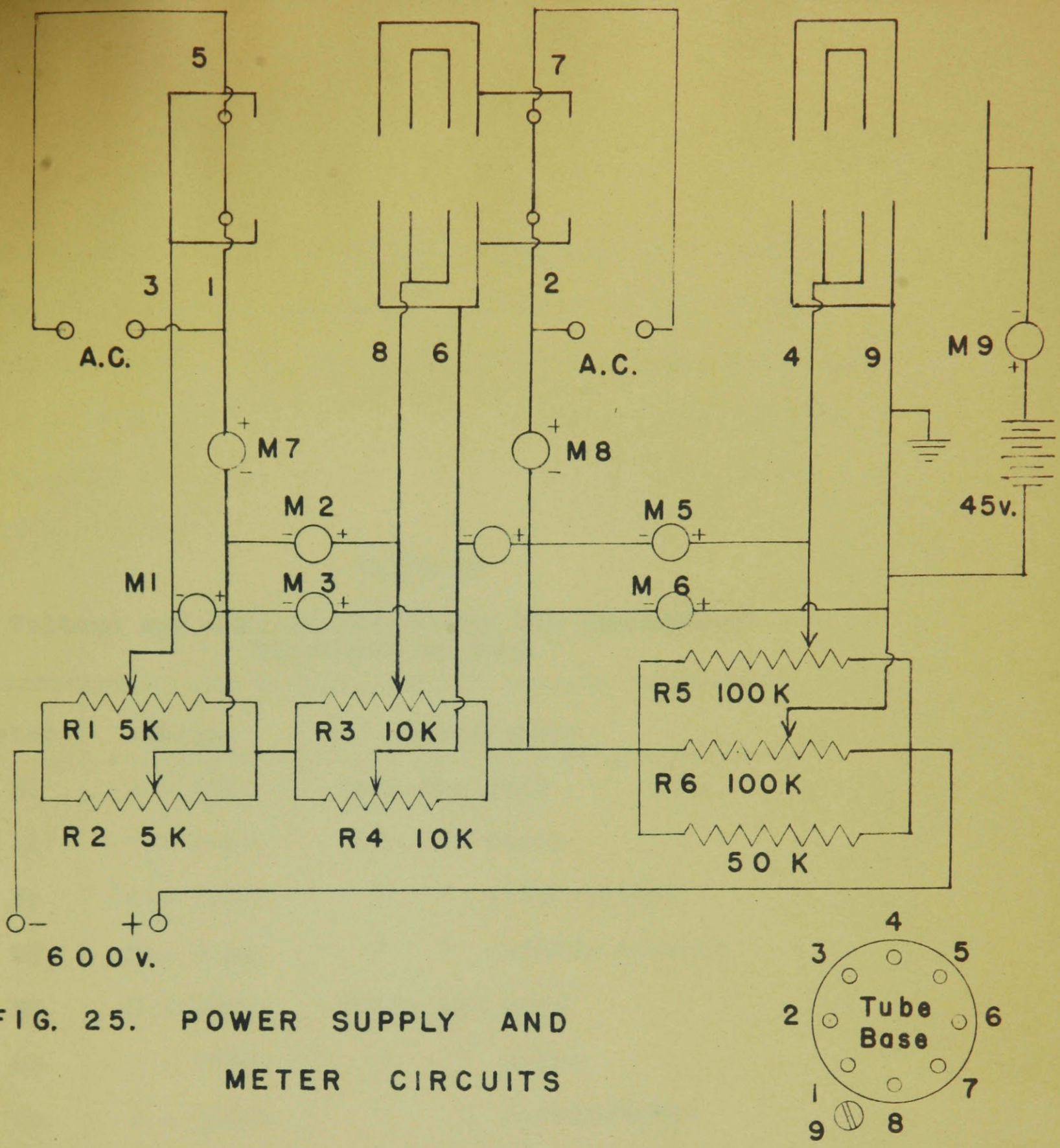

FIG. 25. POWER SUPPLY AND METER CIRCUITS

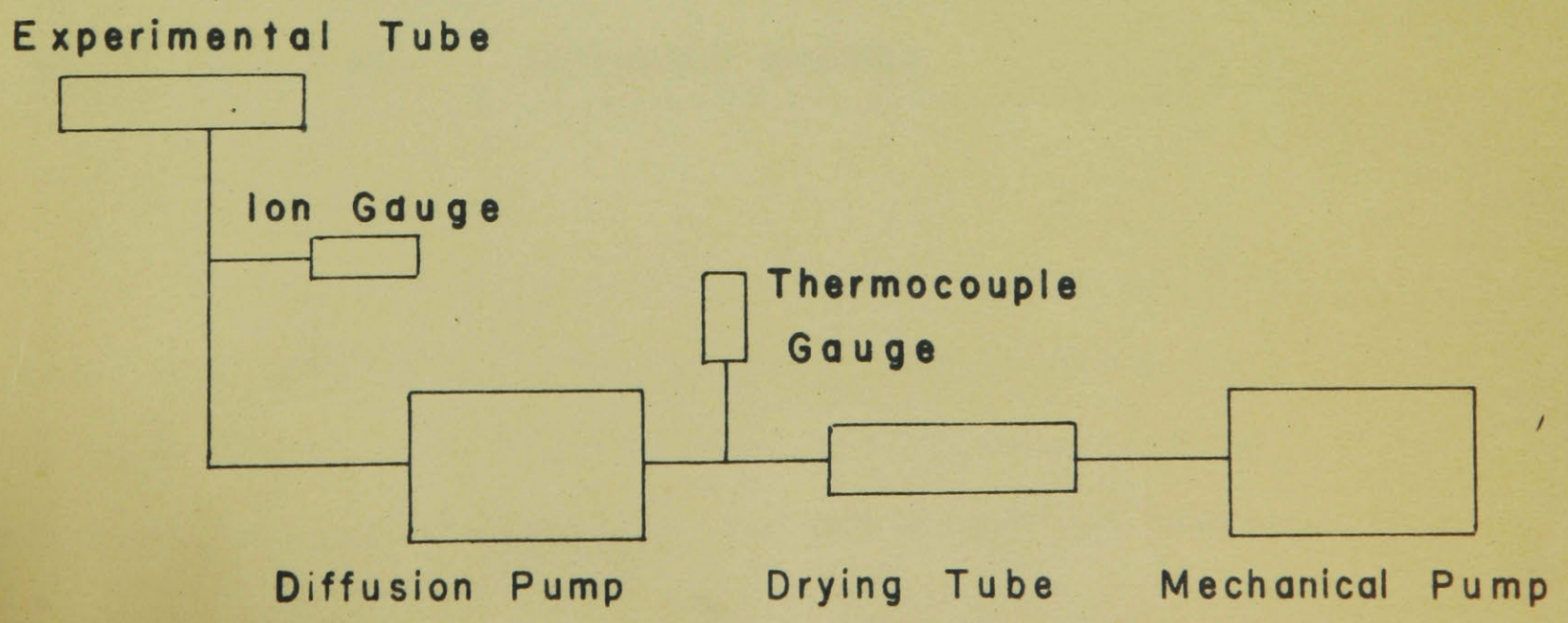

FIG. 24. SCHEMATIC DIAGRAM OF VACUUM SYSTEM

TABLE II

Voltage and Current Meters and the Measurement Performed by Each

Meter	Range	Measurement
M1	0 - 25v.	back gun grid
M2	0 - 100v.	" " focus
M3	0 - 200v.	" " acceleration
M7	0 - 5 ma.	" " cathode current
M4	0 - 25v..	front gun grid
M5	0 - 200v.	" " focus
M6	0 - 500v.	" " acceleration
M8	0 - 5 ma.	" " cathode current
M9	0 - 2 ma.	collector current

back toward the grids of the output resonant cavity. Fig. 26 shows the apparatus arranged on top of the pumping bench. The tube inside the two magnetic coils can be seen at the upper right of the photograph, the ion gauge near the centre, meters on the left, and potentiometers at the lower left.

Electron-Optical Measurements

The initial tests on the electron gun system were made in an evacuated glass tube about thirty inches long. Two means were employed to study the focussing action - small fluroescent screens, and the fluorescence of the gas remaining in the tube at a pressure of about 5×10^{-4} mm. of mercury. In a darkened room, the effect of varying the potentials of the grid cylinders and the ratio of the potentials used in the four aperture lenses could readily be observed. These observations confirmed the predictions of the stroboscopic photographs made on the rubber analogue.

To prepare fluroescent screens, the glass first received a light coating of sulphur from a carbon di-sulphide flame. To this coating finely powdered zinc sulphide, rising from an agitated bottle of the chemical,

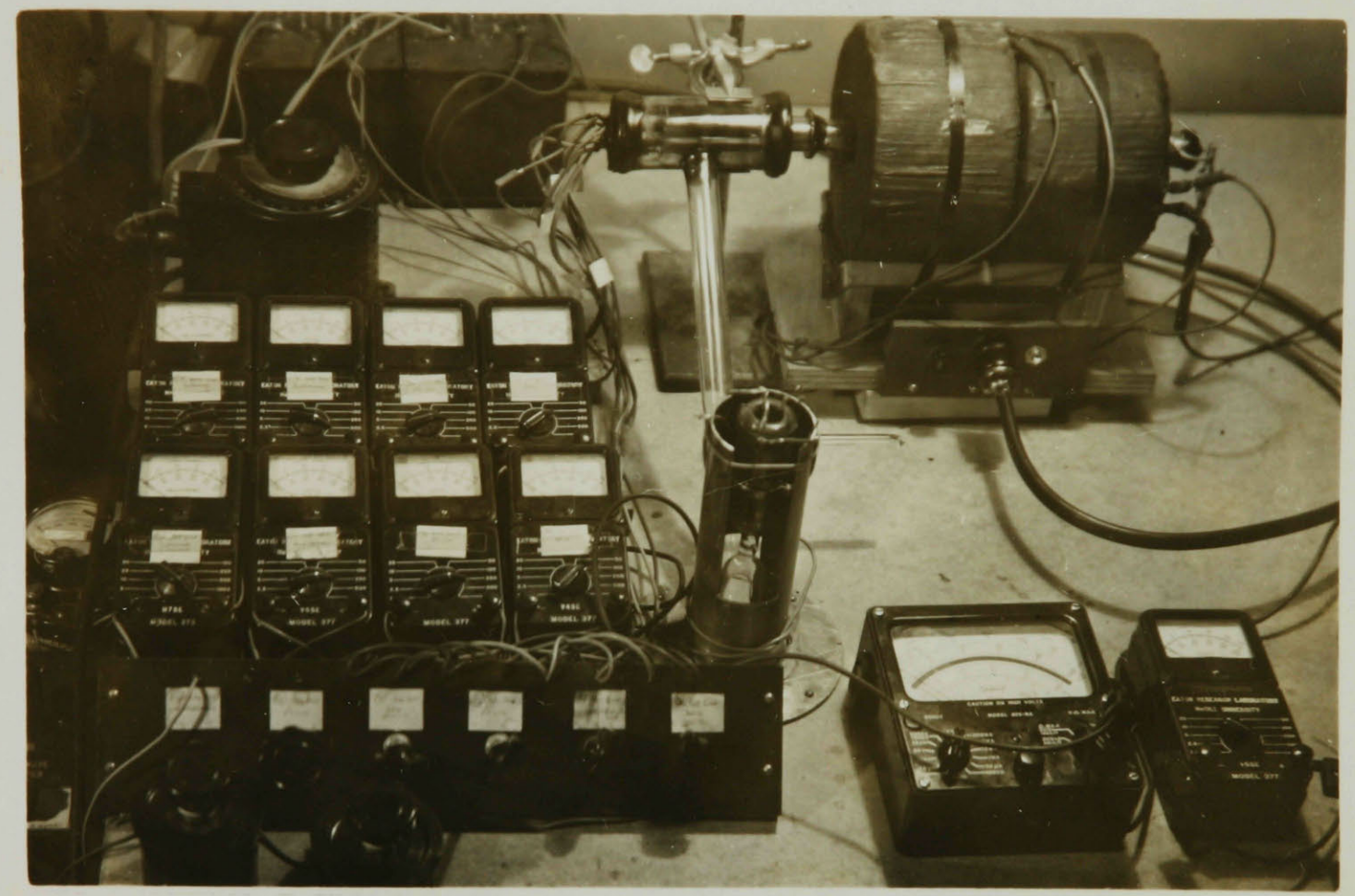

Fig. 26. The Experimental Tube on the Pumping Bench with Meters

adhered. Finally, warming the glass gently drove off the sulphur leaving a layer of zinc sulphide.

In order to determine whether the electron gun system was performing in a satisfactory manner, several pairs of electrical quantities were varied and the results recorded graphically. Two criteria of satisfactory performance were regarded as more important than any others, The first consideration was the ability of the electron-optical system to provide two beams of electrons at the voltages and current densities required by the theoretical design of the double-stream amplifier tube. Secondly, it was desirable to determine whether the beams of electrons were being formed without excessive loss of current to the lens electrodes, and whether these electrodes were exercising the degree of focussing control which the rubber analogue method of design predicted. Fortunately, as it was discovered these two requirements were consistent; the ratio of current in the electron streams to current leaving the cathodes, which has been called the electron-optical efficiency, was higher than is usual in most electron guns.

Separate measurements were made on the front and back sections of the electron gun system, that is, the cathodes were heated only one at a time but voltages

were applied to all electrodes. These measurements were made with the electron guns installed in the complete structure of the amplifier tube with the focussing magnetic coils in place and operating. Those voltages which were not being varied as part of each test were maintained at settings chosen to give the best performance of the system as a whole. The optimum values and the meters in the circuit of Fig. 25 on which they were read, are listed in Table III. In these measurements the values designated as beam current were the currents which actually reached the collector electrode; they registered on meter M9. Thus values of current density computed for the electron streams did not include current lost to the grids of the resonant cavities or other metal parts.

To discover over what range of filament supply voltages the electron emission remained temperature limited, and at what level space-charge limitation set in, the graph of Fig. 27 was plotted. It displays the variation of beam and cathode currents against the setting of the variac which supplied the a.c. filament voltage for the front gun. Below a variac setting of 60 there was no emission. From 65 to 85 the cathode current increased and was temperature limited. Above 85, space-charge limitation occurred and further increase in cathode temperature yielded only a very small

TABLE III

Optimum Values of Voltage for the Electron Gun System

Electrode	Voltage	Meter
Back gun filament	variac at 80	--
" " grid cylinder	-4	M1
" " acceleration	100	M3
" " focussing	32	M2
Front gun filament	variac at 80	--
Front gun grid cylinder	-30	M4
" " acceleration	400	M6
" " focussing	80	M5

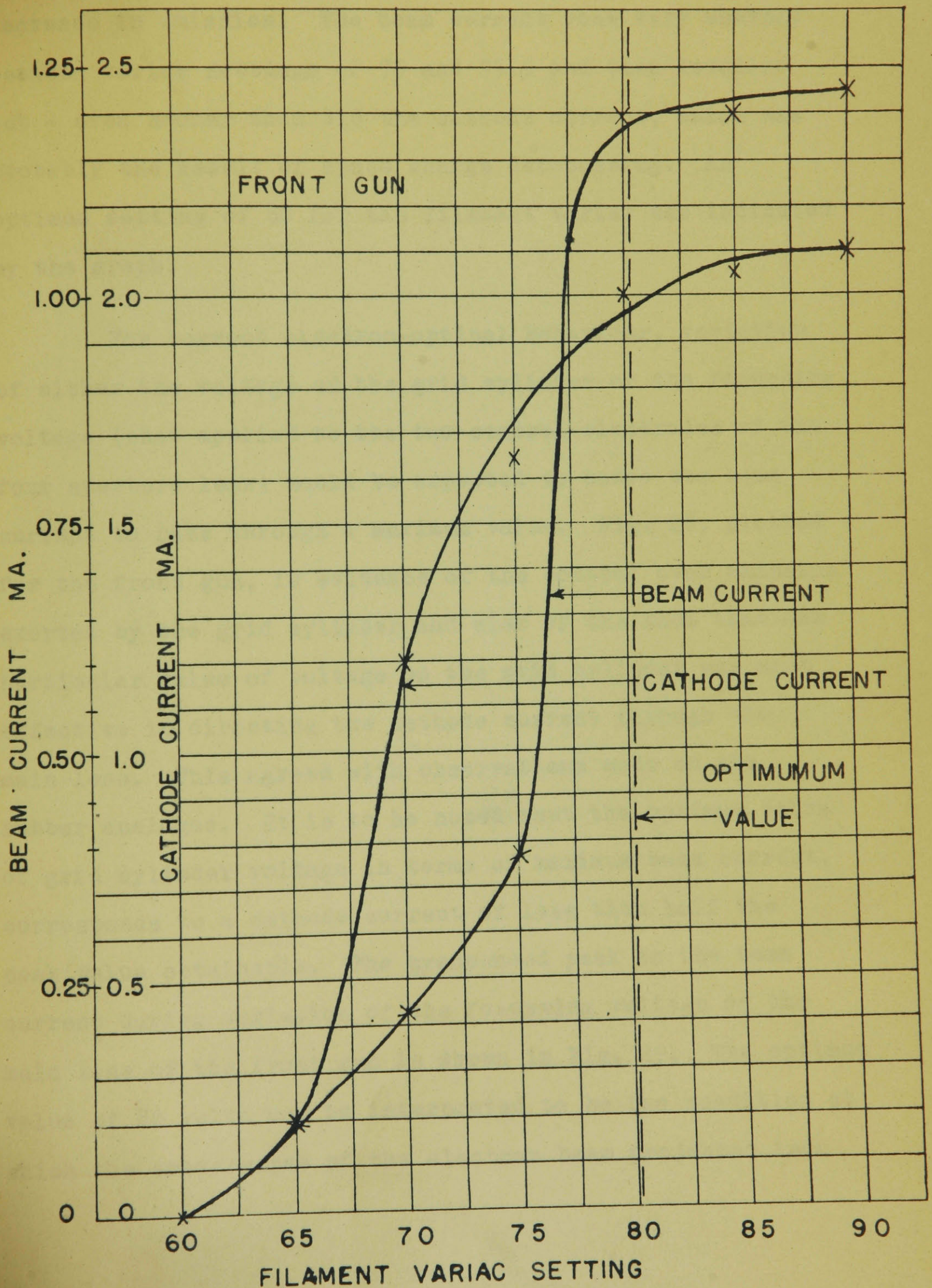
FRONT GUN
BEAM CURRENT
CATHODE CURRENT
OPTIMUMUM
VALUE
BEAM · CURRENT MA.
CATHODE CURRENT MA.
1.25
2.5
1.00
2.0
0.75
1.5
0.50
1.0
0.25
0.5
0
0
60
65
70
75
80
85
90
FILAMENT VARIAC SETTING

FIG. 27

increase in emission. The beam current rose very sharply between variac settings of 75 and 77.5 and then levelled out - even sooner than did the cathode current, which was probably the result of space charge defocussing. An optimum setting of 80 for the filament variac was indicated by the graph.

For correct electron-optical behaviour, variation of either the voltage of the grid cylinder or the focussing voltage (that applied to the two central electrodes of the four aperture lens) would be expected to cause the beam current to pass through a maximum value. Fig. 28, plotted for the front gun, is evidence of the control over emission exerted by the grid cylinder and also of the fact that one particular value of voltage on the grid cylinder was most effective in directing the cathode current through the main lens. This agreed with observations made on the rubber analogue. It is to be noted that the optimum value of grid cylinder voltage in terms of maximum beam current, corresponds to a cathode current of less than half the peak value obtainable. The pronounced peak in the beam current during variation of the focussing voltage of the main lens of the front gun is shown in Fig. 29. The optimum value of 80 volts may be interpreted to be the condition at which the convergence of the electron beam projected into

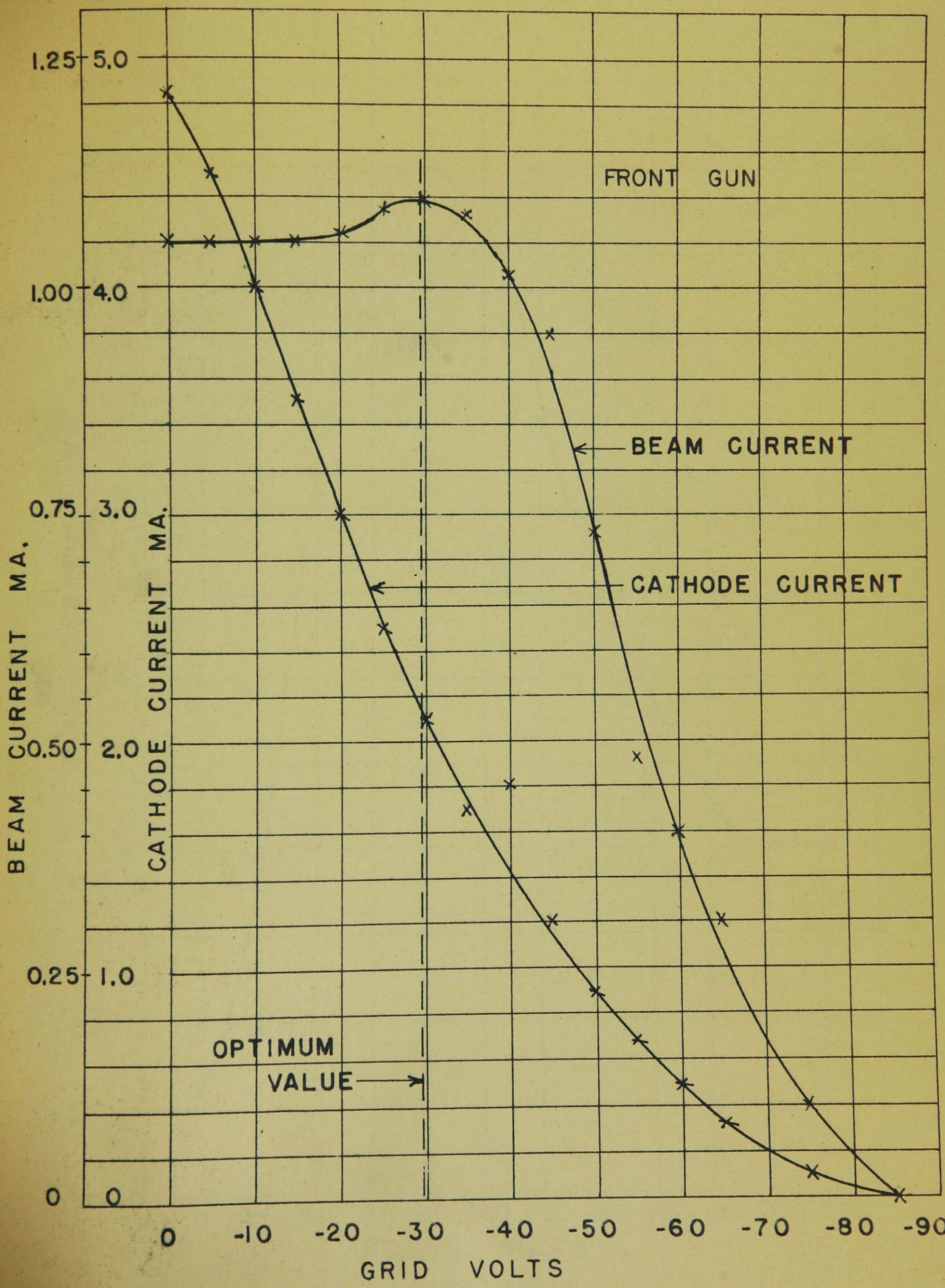
1.25
5.0
1.00
4.0
0.75
3.0
0.50
2.0
0.25
1.0
0
0
BEAM CURRENT MA.
CATHODE CURRENT MA.
FRONT GUN
BEAM CURRENT
CATHODE CURRENT
OPTIMUM VALUE
0
-10
-20
-30
-40
-50
-60
-70
-80
-90
GRID VOLTS

FIG. 28.

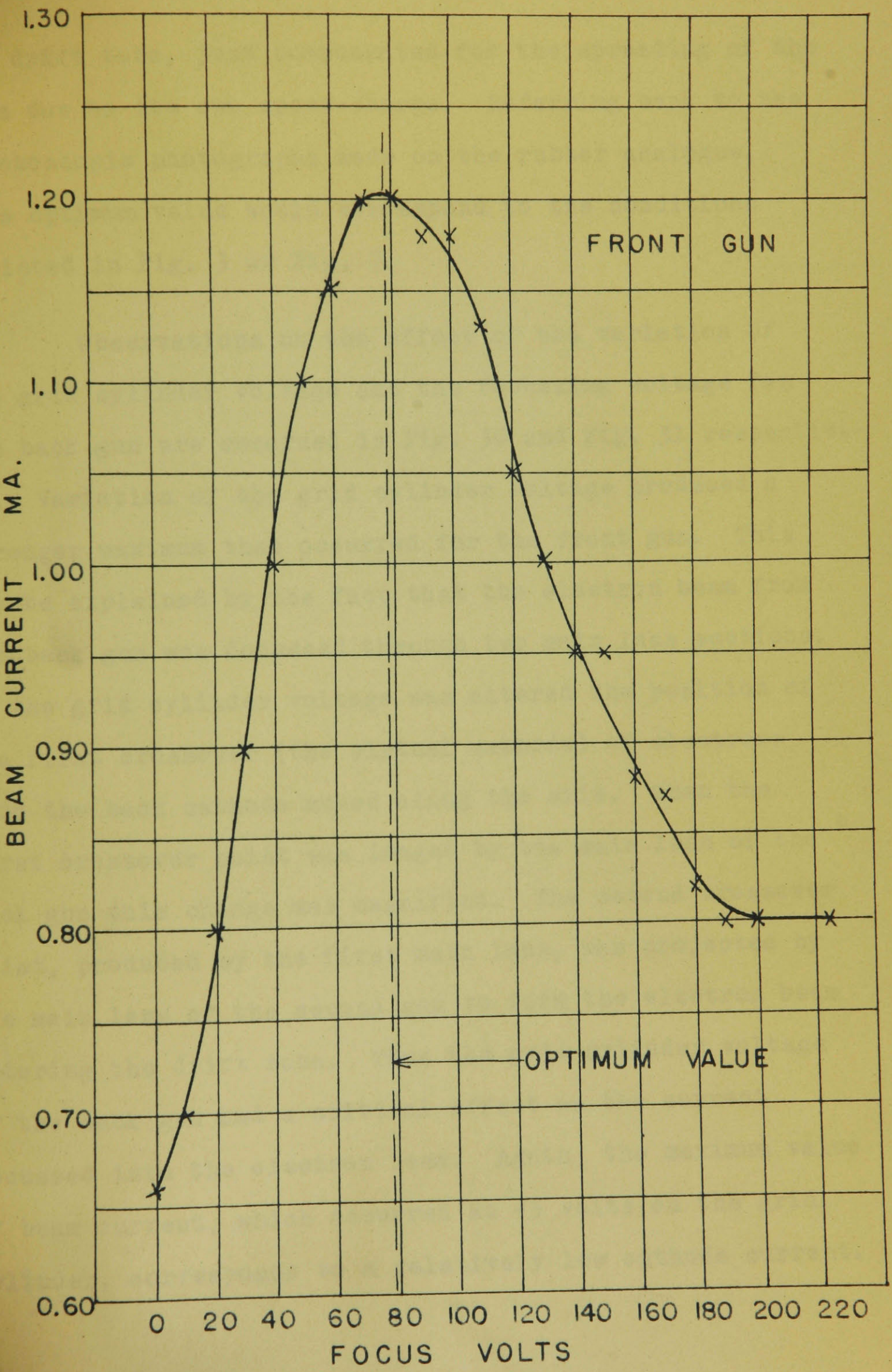
1.30
1.20
1.10
1.00
0.90
0.80
0.70
0.60
BEAM CURRENT MA.
FRONT GUN
OPTIMUM VALUE
0 20 40 60 80 100 120 140 160 180 200 220
FOCUS VOLTS

FIG. 29.

the drift tube, just compensated for the spreading of the beam due to its own space-charge. Referring back to the stroboscopic photographs made on the rubber analogue, this optimum value would correspond to the conditions depicted in Fig. 3 or Fig. 7.

Observations on the effect of the variation of the grid cylinder voltage and the focussing voltage for the back gun are recorded in Fig. 30 and Fig. 31 respectively. Variation of the grid cylinder voltage produced a stronger maximum than occurred for the front gun. This may be explained by the fact that the electron beam from the back gun was focussed through two main lens sections. As the grid cylinder voltage was altered the position of the first crossover (the virtual cathode) of electrons from the back cathode moved along the axis. When the first crossover point was imaged by the main lens of the back gun this change was magnified. The second crossover point, produced by the first main lens, was projected by the main lens of the second gun to form the electron beam entering the drift tube. Thus the grid cylinder voltage of the back gun had a critical effect on the current focussed into the electron beam. Again, the maximum value of beam current, which occurred at -3 volts on the grid cylinder, corresponds to a relatively low cathode current.

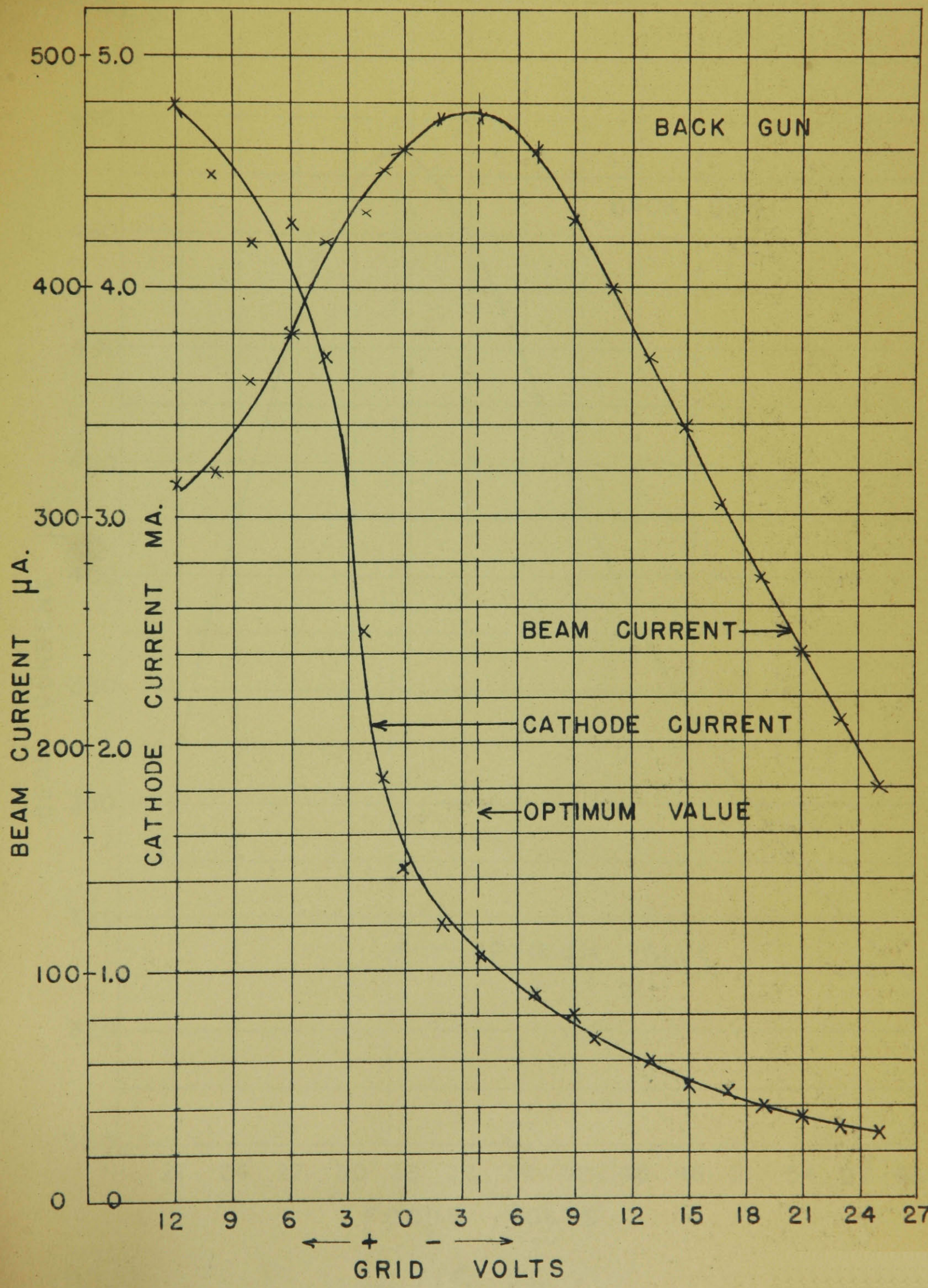
BACK GUN
BEAM CURRENT
CATHODE CURRENT
OPTIMUM VALUE
BEAM CURRENT μA.
CATHODE CURRENT MA.
500
400
300
200
100
0
5.0
4.0
3.0
2.0
1.0
0
12 9 6 3 0 3 6 9 12 15 18 21 24 27
+
−
GRID VOLTS

FIG. 30.

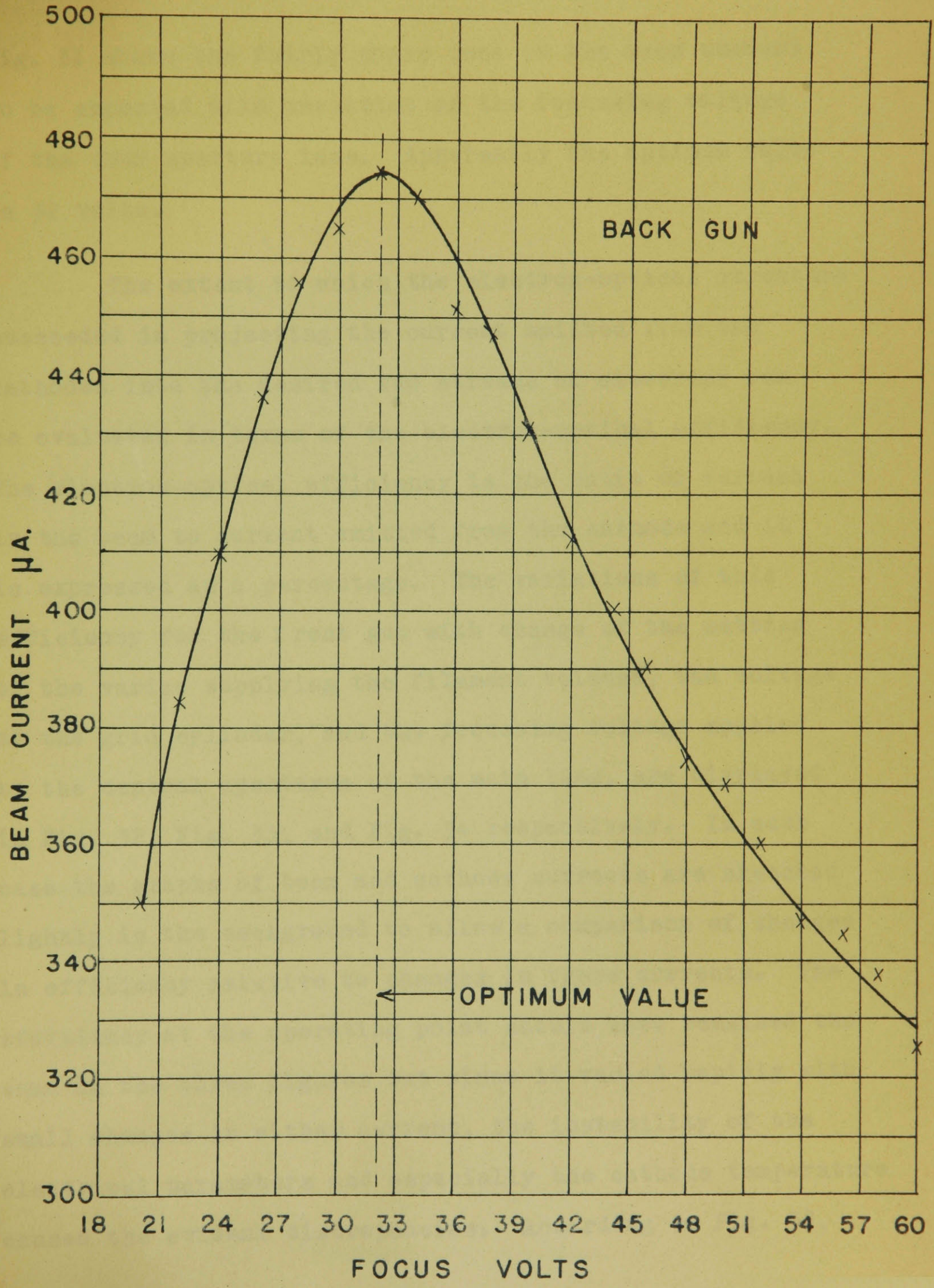
BACK GUN
OPTIMUM VALUE
BEAM CURRENT μA.
500
480
460
440
420
400
380
360
340
320
300
18
21
24
27
30
33
36
39
42
45
48
51
54
57
60
FOCUS VOLTS

FIG. 31.

Fig. 31 shows the fairly sharp peak in the beam current to be expected with variation of the focussing voltage of the four aperture lens. Apparently the optimum value is 32 volts.

The extent to which the electron-optical structure succeeded in projecting the current emitted from the cathodes into the desired two streams of electrons can be evaluated in terms of the electron-optical efficiency. The electron-optical efficiency is the ratio of current in the beam to current emitted from the cathode and it is expressed as a percentage. The variations of this efficiency for the front gun with change of the setting of the variac supplying the filament voltage, the voltage of the grid cylinder, and the focussing voltage applied to the central apertures of the main lens, are displayed in Fig. 32, Fig. 33, and Fig. 34 respectively. In each case the graphs of beam and cathode currents are sketched lightly in the background to allow a comparison of changes in efficiency relative to changes in these currents. The efficiency at the operating point should have remained the same on the three figures but since it varied rapidly with small changes in either current, the instability of the electrical parameters and especially the cathode temperature caused the evident discrepancies. According to Fig. 32,

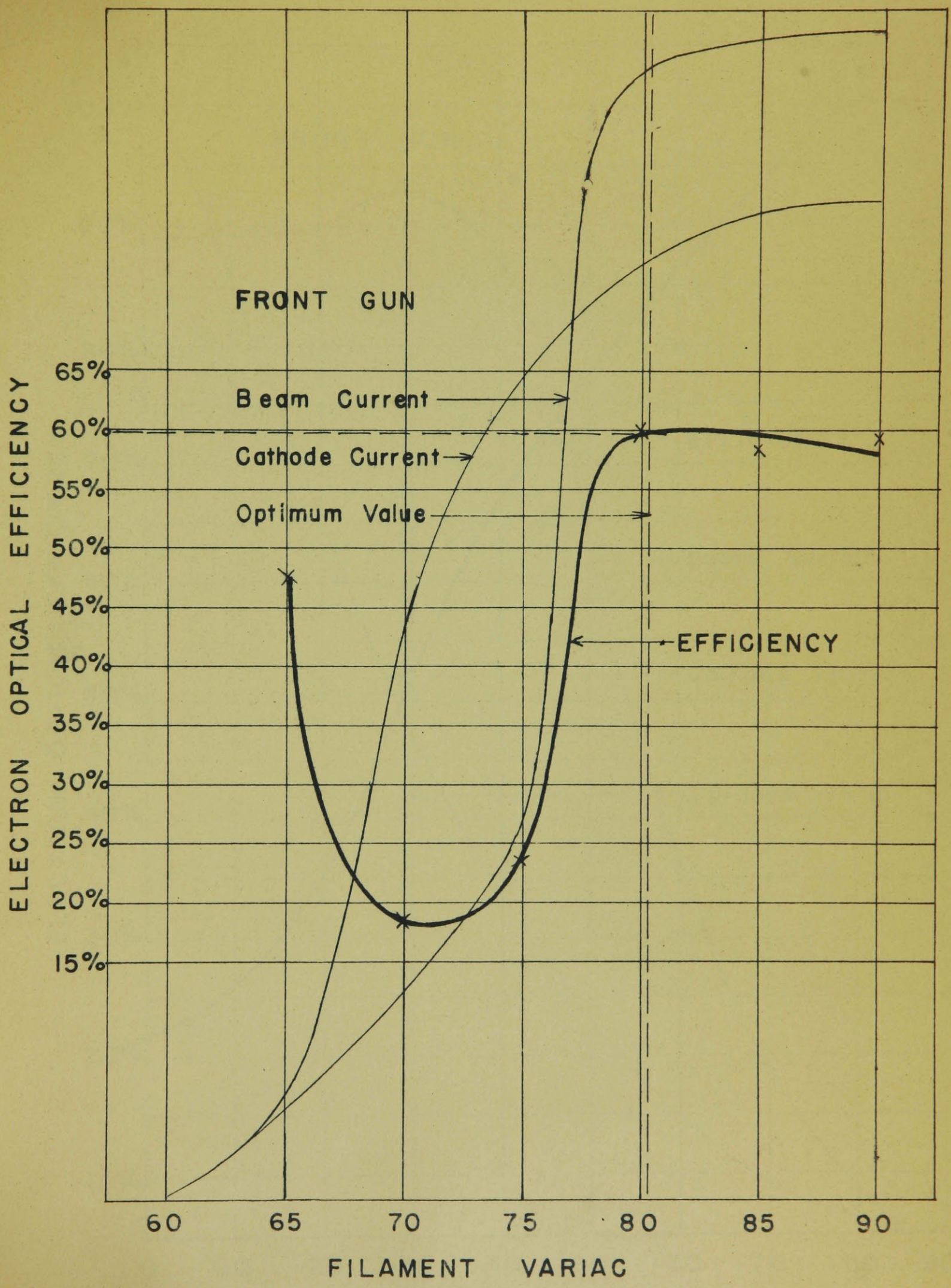
FRONT GUN
Beam Current
Cathode Current
Optimum Value
EFFICIENCY
ELECTRON OPTICAL EFFICIENCY
65%
60%
55%
50%
45%
40%
35%
30%
25%
20%
15%
60
65
70
75
80
85
90
FILAMENT VARIAC

FIG. 32.

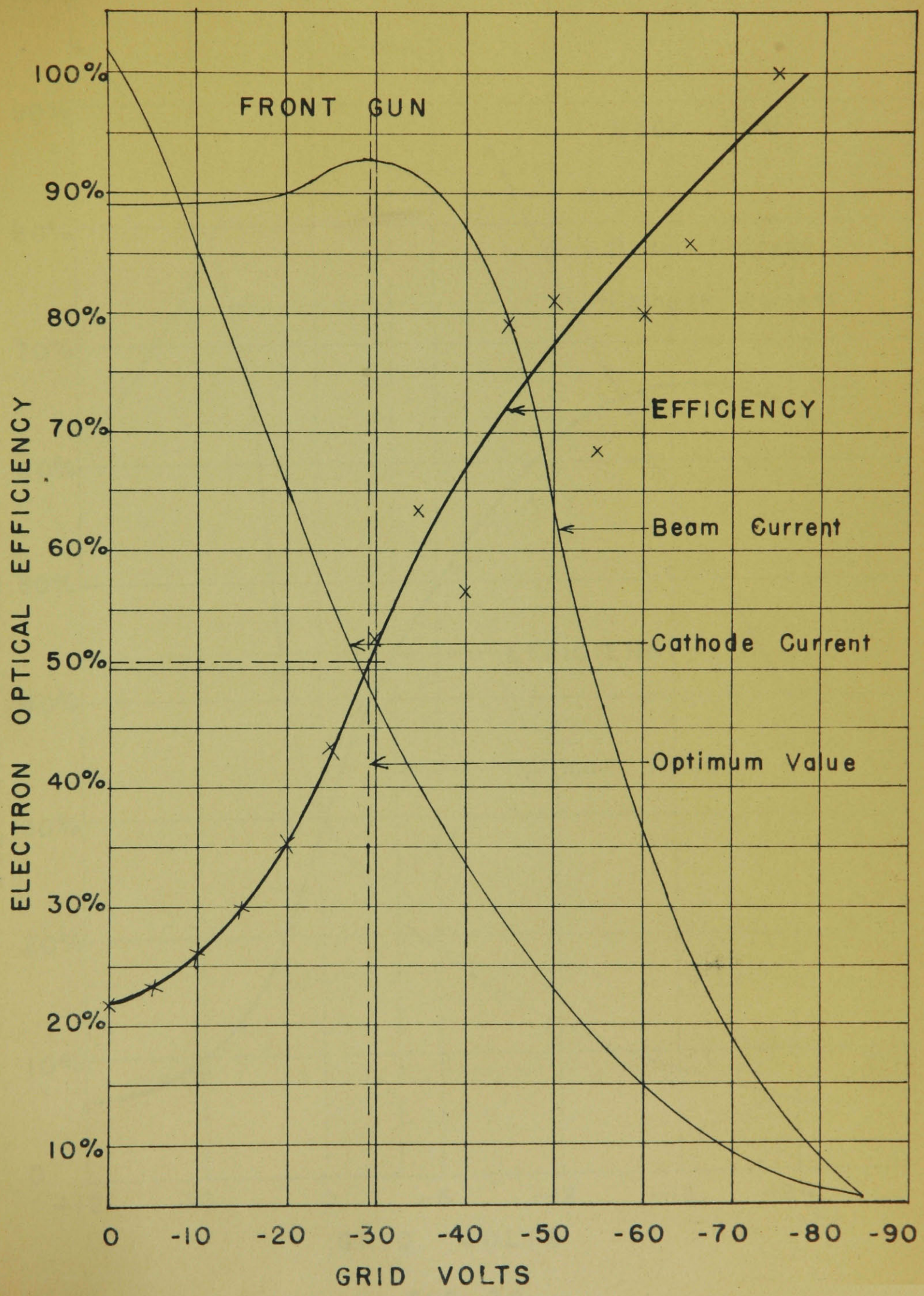
FRONT GUN
EFFICIENCY
Beam Current
Cathode Current
Optimum Value
ELECTRON OPTICAL EFFICIENCY
100%
90%
80%
70%
60%
50%
40%
30%
20%
10%
0
-10
-20
-30
-40
-50
-60
-70
-80
-90
GRID VOLTS

FIG. 33.

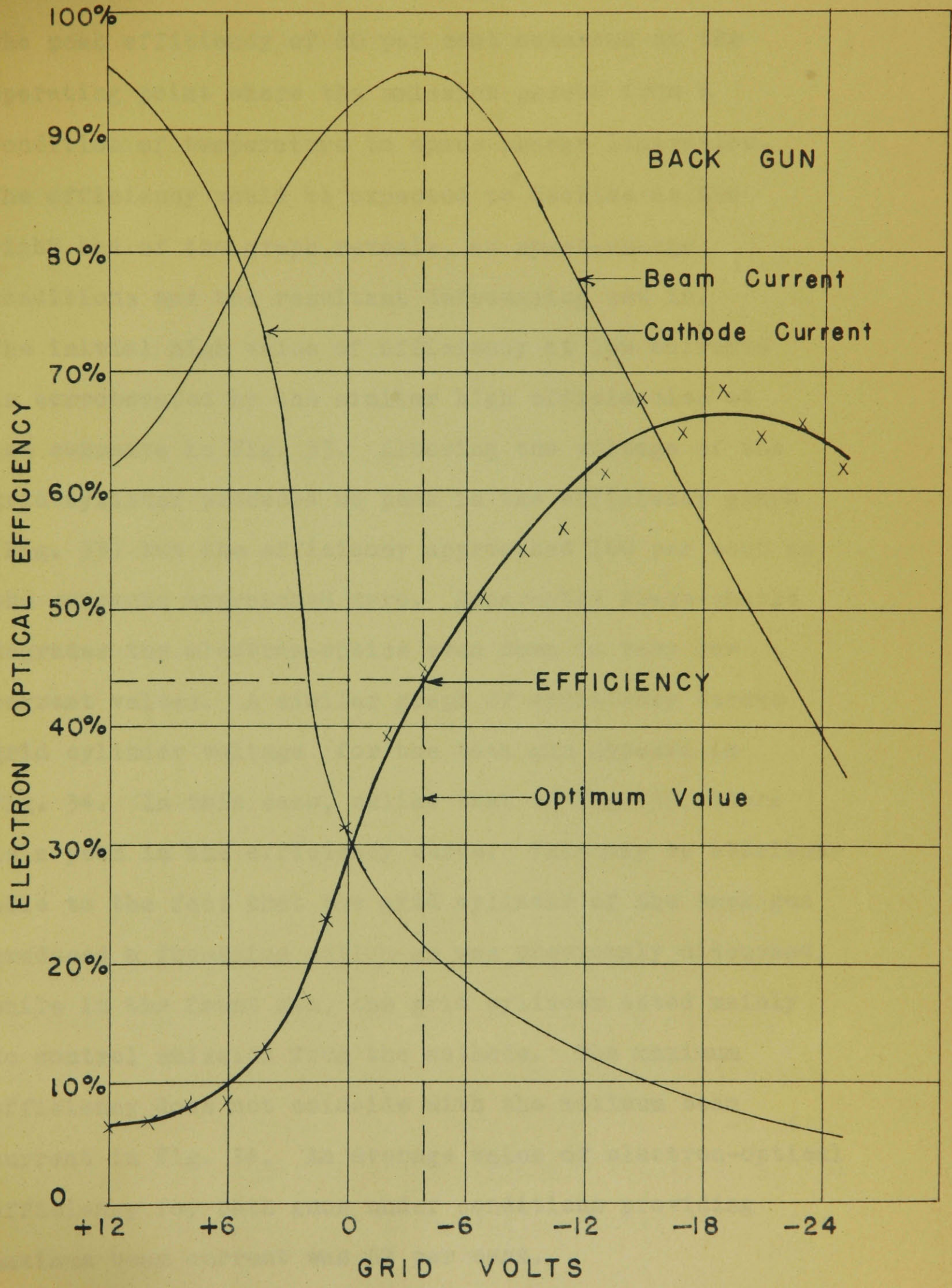
100%
90%
80%
70%
60%
50%
40%
30%
20%
10%
0
ELECTRON OPTICAL EFFICIENCY
BACK GUN
Beam Current
Cathode Current
EFFICIENCY
Optimum Value
+12
+6
0
-6
-12
-18
-24
GRID VOLTS

FIG. 34.

the peak efficiency of 60 per cent occurred at the operating point where the emission passed from a condition of temperature to space charge limitation. The efficiency would be expected to decline as the right end of the graph reveals, as space-charge conditions and the resultant defocussing set in. The initial high value of efficiency at low currents is corroborated by the similar high efficiencies at low currents in Fig. 33. Altering the voltage of the grid cylinder produced no peak in the efficiency graph (Fig. 33) but the efficiency approached 100 per cent as the currents approached zero. Apparently space-charge degrades the electron-optics even down to very low current values. A similar graph of efficiency versus grid cylinder voltage for the back gun appears in Fig. 34. In this case, unlike that of Fig. 33, there is a peak in the efficiency curve. This may be attributable to the fact that the grid cylinder of the back gun produced a focussing action as was previously discussed, while in the front gun, the grid cylinder acted mainly to control emission from the cathode. The maximum efficiency does not coincide with the maximum beam current in Fig. 34. An average value of electron-optical efficiency for both guns under conditions providing maximum beam current was 52 per cent.

RADIO FREQUENCY MEASUREMENTS

The measurements on the performance of the experimental double-stream amplifier tube were made using a r.f. signal generator (operating c.w.) and a microwave receiver. The receiver and its power supply are shown in the photograph Fig. 35. The tuning range of the receiver was from 8.0 to 11.0 cm.; the manual of operation recommended a setting of 10.7 cm. Using a coaxial wavemeter equipped with crystal output probe, an audio amplifier, and output current meter, the signal generator was set up accurately on 10.70 cm. The signal generator is displayed in Fig. 36 appearing on the right of the photograph while the audio amplifier and the wavemeter are on the left and in the foreground respectively. The receiver was tuned to 10.7 cm. while connected directly to the signal generator.

With the apparatus arranged as shown in Fig. 37 the resonant cavities were tuned to 10.7 cm. and the receiver tuning adjustments were checked for optimum setting. After the tube had been evacuated the electron gun system and magnetic coils were turned on and adjusted to give maximum current to the collector electrode at the far end of the tube. All else seeming satisfactory, the

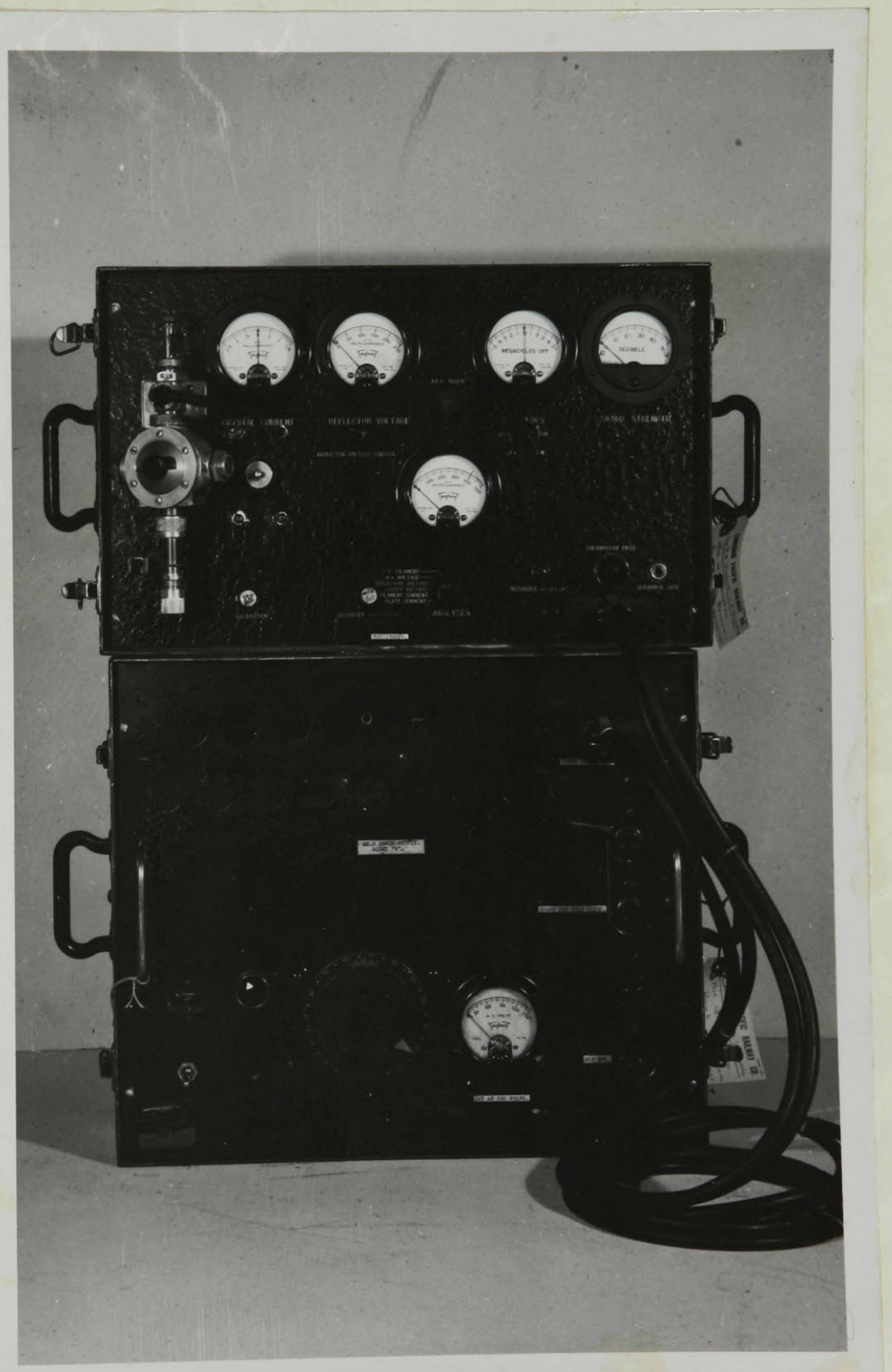

Fig. 35. Microwave Receiver and Power Supply

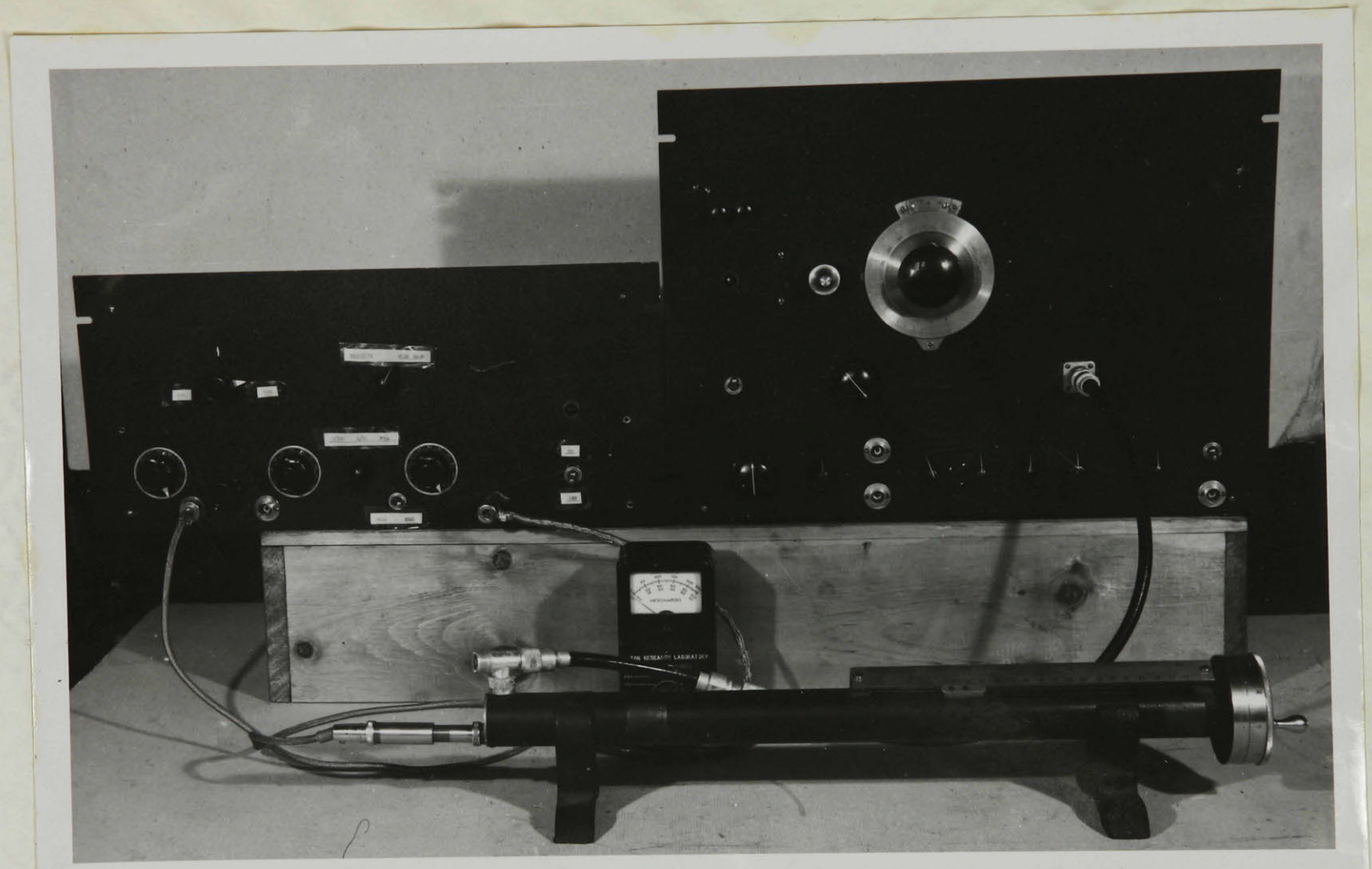

Fig. 36. Signal Generator, Audio Amplifier and Wavemeter

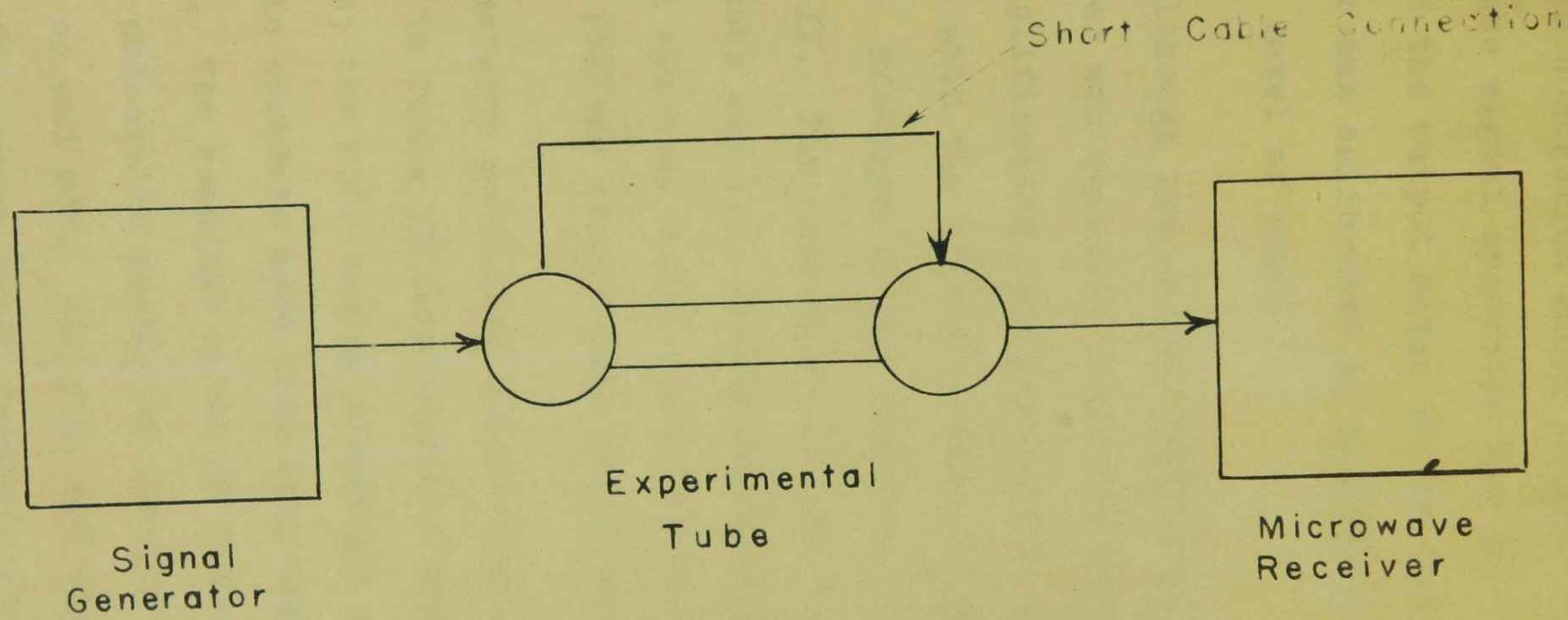

FIG. 37. THE ARRANGEMENT OF APPARATUS FOR RADIO FREQUENCY TESTS

short cable connection shown in Fig. 37 was broken at point A, the signal generator was set to provide full power, and the output meter of the receiver was observed. This meter was calibrated in decibels above an arbitrary reference level of power.

Although the overall gain from signal generator to receiver was actually negative, evidence of the double-stream amplification phenomenon was obtained. Observations were made with the electron beams present separately and together. Readings of the receiver output meter are listed in Table IV. The method was to set the various voltages and currents and r.f. tuning adjustments for maximum output with both electron beams turned on and to retain these settings for the single beam readings.

Several pertinent observations can be listed. The readings in Table IV were repeated several times on different occasions; the r.f. tuning procedure and the setting of the electronic controls were done over again and the readings were the same. The readings given in Table IV could be repeated in rapid succession merely by turning the filament heater voltages on and off. All r.f. and electronic controls affected the output meter reading, giving a maximum output at one particular setting. With both electron beams on, changing the filament temperatures by means of the variacs

TABLE IV

Radio Frequency Measurements Made on the Double-Stream Amplifier

Electron Beam	Receiver Meter Reading
Front gun alone	6 db.
Back gun alone	11 db.
Both guns together	19 db.

which supplied the heating voltages, produced an optimum setting which did not correspond with highest temperature nor with maximum beam current. With both electron beams on, one of the filaments could be reduced to a low temperature (from a dazzling white down to a bright red) before the output reading dropped appreciably below the 19 db. figure. Changing the voltage ratio of the two electron beams caused the output meter to show a succession of peaks which were reproducible. Again greatest r.f. output did not coincide with highest current in the electron beams. When either beam was used alone the setting for maximum signal output always coincided with that for maximum beam current. The signal output for a single beam was not affected by a change in voltage so long as the total beam current was held constant by adjustment of the filament temperature. All readings listed in Table IV are conservative; on one occasion with both beams on, the output reading reached 29 db. but was very unstable and could not be recovered.

A Comparison of the Readings Recorded in Table IV

Let Pr be the unknown power reference level for which the receiver output meter is calibrated in decibels.

Let Pf = power output using the front gun alone

Pb = power output using the back gun alone

Ps = the power output which was actually present using both electron guns.

The readings in Table IV give the three equations following.

$$10 \log Pf/Pr = 6 \quad \text{or} \quad Pf = Pr10^{0.6} \tag{24}$$

$$10 \log Pb/Pr = 11 \quad \text{or} \quad Pb = Pr10^{1.1} \tag{25}$$

$$10 \log Ps/Pr = 19 \quad \text{or} \quad Ps = Pr10^{1.9} \tag{26}$$

It is desired to compare the sum of the separate electron beam output powers Pf and Pb with Ps, the power actually observed with the beams on together. It must be noted that it is not permissible merely to add the 6 db. and 11 db. figures because the two electron beams were operating in parallel and not in series. Only if the output of one beam became the input of the other, would the total gain be the arithmetic sum of the two db. readings.

The power coupled to a resonant cavity presenting a voltage V to a beam of electrons of current I, with a beam coupling coefficient A, is P = AIV. In reality V depends on the cavity impedance, which is lowered by the presence of an electron beam. Here it is assumed that the resonator voltage for a single beam was not lowered when the other beam was

turned on. This effect may actually have been negligible in comparison with other heavy losses of radio frequency energy.

Furthermore, the signal wavelengths in the electron beams depend on beam voltages. Since the beams were many wavelengths long the total signal at the end of the beams might have varied from the sum to the difference of the individual signal values depending on their relative phase. A sample calculation is made in Appendix I.

$$\frac{Ps}{Pf \pm Pb} = \frac{Pr10^{1.9}}{Pr\,(10^{0.6} \pm 10^{1.1})} = 4.8 \text{ or } 9.2 \qquad (27)$$

Expressed in decibels this becomes

$$10 \log Ps/\,(Pf \pm Pb) = 6.8 \text{ db. or } 9.6 \text{ db.} \qquad (28)$$

This means that even if the two separate beams are considered to have added their output signals in phase, there was still an improvement of 6.8 db. in the observed value of output power for both beams together over the total of the observed values for the beams acting separately. It may be concluded that this improvement is attributable to the presence of the phenomenon of double-stream amplification.

Discussion of the Reasons for Energy Losses

The fact that the overall gain of the experimental tube was negative in spite of the amplification present suggests that considerable loss of radio frequency energy took place.

The major loss of power may be blamed on the impedance mismatches between the r.f. cables and the resonant cavities used on the tube. No matching devices were used so that a large standing wave ratio was presumably present in the cables resulting in poor energy transfer to and from the cavities.

A second loss of power was that due to the low Q of the resonant cavities. Two factors contributed to this low Q. Firstly, there was a considerable quantity of glass and vacuum sealing wax inside the cavities. Secondly, it was necessary to turn in the threaded tuning plugs in the cavities to almost their extreme depth in order to produce resonance at 10.7 cm. In this condition the fields inside the cavity were highly distorted, the ratio of cavity surface to volume was increased and the input and output loops to the r.f. cables were poorly coupled. The low Q of the resonators was apparent in their very broad tuning response.

A small part of the total energy loss was ~~the~~ the result of the less than ideal beam coupling coefficients at the resonant cavities. This accounts for a loss of approximately 1.6 db. Calculations are presented in Appendix II.

SUMMARY

A new type of amplifier suitable for the amplification of frequencies in the microwave region has been described. This type of amplifier is able to produce amplification by a process of the interaction of space-charge waves travelling along two superimposed beams of electrons. The theoretical analysis predicted that under certain conditions of voltages and current densities of the two electron streams, there would be set up a wave increasing exponentially with distance. This analysis has led to the calculation of values of the various parameters involved in the construction of an experimental tube.

The major problem dealt with in this report has been the design and construction of an electron gun system able to provide two superimposed streams of electrons having the voltages and current densities required. The device which was built, consisted of two electron guns mounted one behind the other on a common axis of cylindrical symmetry and having the front gun section transparent to the beam from the back gun. This electron-optical system was built on the basis of observations and stroboscopic photographs made on a rubber membrane analogue

of the electrode configuration. Measurements made on the completed electron gun system, of its general behaviour and the control exercised by the various electrodes, confirmed the predictions of the rubber model. Thus the rubber membrane analogue method has been demonstrated to be of great value in the design of electron-optical devices of this sort.

The experimental tube was built in a demountable form. The interchange of energy between the radio frequency circuits and the electron streams at the input and output of the amplifier tube, took place in resonant cavities each equipped with a closely spaced pair of grids through which the electron streams passed. Lack of proper impedance matching between the cavities and the connecting cables apparently resulted in a large loss of energy.

Radio frequency tests made at a wavelength of 10.7 cm., have provided evidence of the existence of the phenomenon of double-stream amplification. The overall gain of the experimental tube was negative and no measurement of the various energy losses believed due to impedance mismatches and low Q cavities, nor of the gain in the electron streams independently of these circuit losses, has been possible.

Little attention has been paid to the value of the double-stream tube as a practical amplifier. The construction of the tube and the performance of measurements have been undertaken only from an experimental viewpoint. A factor of prime practical importance which is still unknown is the noise figure. Certainly experimental investigation and engineering development may be expected to be in progress in the Laboratories whose scientists' names make up the list of references here included. The hope that double-stream amplifiers may eventually operate satisfactorily even at the short millimetre wavelengths is a promising one.

ACKNOWLEDGEMENTS

The author wishes to express his gratitude to several persons who have given assistance with this project. The investigation of double-stream amplifiers was shared by a group of three graduate students under the supervision of Professor G.A. Woonton. Mr. C.R. Crowell was concerned with the design and construction of radio frequency equipment, particularly a good 10 cm. signal generator, suitable for the evaluation of the performance of the experimental tube. Mr. G. Bekefi undertook an advanced analysis of the theory of double-stream amplification. In the work described in this report the author received from these two fellow students both practical assistance and the benefit of frequent discussions. The 35 mm. camera used for the rubber analogue photographs was loaned by Mr. H.D. Griffiths. The microwave receiver employed to make radio frequency measurements was provided by the National Research Council, Ottawa, through the generous cooperation of Dr. G.A. Miller. This work has been carried out with the assistance of a scholarship granted by the Research Council of Ontario, to whom the author is particularly grateful.

APPENDIX I

The Calculation of Wavelengths in the Electron Streams

To calculate wavelengths in the electron streams use is made of the relation

$$\text{Transit angle} = T = 1000\pi\ell / V^{1/2} \; Y \text{ radians} \qquad (29)$$

as given in Spangenberg's text (2) page 550 where

T = transit angle in radians

ℓ = distance beam travels during T

V = d.c. beam accelerating voltage

Y = signal wavelength.

When $T = 2\pi$, ℓ becomes the wavelength in the electron stream and is given by

$$Ys = \ell = V_o^{1/2} \; Y/500 \qquad (30)$$

Thus knowing the signal wavelength (Y = 10.7 cm.) and the beam voltages the wavelengths in the beams can be calculated. For the 500 volt beam Ys = 0.479 cm. and for the 400 volt beam Ys = 0.428 cm. The numbers of cycles in the 25 cm. drift tube are 52.2 and 58.4 for the faster and slower beams, respectively. Therefore, the two signals if considered to be carried by the beams separately, would be out of phase by 0.4 - 0.2 = 0.2 cycles = 72°. This phase difference cannot, however, be used for any accurate calculations because it varies rapidly with a small change in either beam voltage and these voltages were measured on rather inaccurate voltmeters.

APPENDIX II

Calculation of Beam Coupling Coefficients

Beam coupling coefficient A is given by (reference 8 page 540)

$$A = \frac{\sin T/2}{T/2} \qquad (31)$$

where T is the intergrid transit angle used in Appendix I.

$$T = 1000 \pi \ell / V_o^{1/2} Y \qquad (29)$$

The intergrid spacing was ℓ = 0.152 cm. and the signal wavelength Y = 10.7 cm.

For the front gun V = 400 volts so that T becomes 128° and A is 0.810. For the back gun V = 500 volts so that T is 114° and A equals 0.844.

The overall beam coupling coefficient including input and output circuits is A^2, so that using an average value of A = 0.827 we obtain

$$A^2 = 0.684$$

Expressed in decibels this becomes

10 log 1/0.684 = 1.64 db. (32)

This is the power loss to be expected due to the finite transit time of the electron beam through the resonator grids.

APPENDIX III

An Evaluation of Conditions Present in the Tube as Compared with the Theoretical Optimum

It will be shown that the currents and voltages used satisfied the conditions for double-stream amplification to occur and further, that no change in currents or voltages would have resulted in any appreciable increase in gain. The calculations are based on an article by J.R. Pierce and W.B. Hebenstreit (4). Their notation as well as numbers designating equations and graphs will be used here as far as possible.

Calculation of Critical Current Density

Assume beam radius = a = 0.2 cm. [x]. J^1 and V^1 are mean values of current density and beam voltage defined by

$$J_1/V_1^{3/2} = J_2/V_2^{3/2} = J^1/V^{1\,3/2} \qquad (12a)$$

V_1 = 500 volts. V_2 = 400 volts. Let V^1 = 450 volts.

Fractional velocity separation is

$$b = 2(u_1 - u_2) / (u_1 + u_2) = 2(V_1^{1/2} - V_2^{1/2}) / (V_1^{1/2} + V_2^{1/2})$$
$$= 0.1135 \qquad (6)$$

---

[x] The final aperture of the electron gun had a radius of 0.3 cm. but most of the current appeared to have been confined to a smaller crossection. At any rate, since minimum critical current varies inversely with a, the value a = 0.2 cm. is a conservative choice.

Signal wavelength in the electron stream is

$$Ys = 1.98 \times 10^{-3} \; Y \; V^{1} \; 1/2 \qquad (26)$$

$$= 0.45 \text{ cm.}$$

Therefore, $a/Ys = 0.444$

From Fig. 4 (reference 4) with $a/Y s = 0.444$

obtain $\left[\frac{Wm}{b}\right]^2 = 0.2$ and $Wm^2 = 0.00257$

where Wm is the critical minimum value of W to produce double-stream amplification and in general

$$W^2 = 8.52 \times 10^{6} \; J^{1}/f \; V^{1} \; 1/2 \qquad (28)$$

where f = signal frequency in megacycles = 2800 and J^1 is expressed in amperes per square centimetre. Now this value of Wm, used in equation 28, gives the minimum current density J^1m that will produce double-stream gain:

$$J^1m = 0.02 \text{ ma./cm.}^2$$

Calculation of Gain

Next consider the conditions which were actually present in the experimental tube. The currents used in the beams averaged 0.8 ma. which gives a current density of

$$J^1 = 0.8/\pi a^2 = 6.37 \text{ ma./cm.}^2$$

(This is more than 300 times greater than the necessary minimum value).

The value of W^2 from equation 28 is

$$W^2 = 0.915$$

Thus $(W/Wm)^2 = 0.915/0.00257 = 356$

Fig. 3 of reference 4 displays the variation of Db. gain/wavelength/unit b as a function of $(W/Wm)^2$. In this case with $(W/Wm)^2 = 356$ the reading is above 27.2 db./wavelength/unit b.

Since the maximum value possible under any condition is 27.3 db./wavelength/unit b, it can be concluded that the voltages and currents used could not have been changed to any appreciable advantage.

REFERENCES

1. HAEFF, A.V. The electron wave tube - a novel method of generation and amplification of microwave energy. Proc. I.R.E. 7: 4-10. 1949.

2. HOLLENBERG, A.V. Experimental observation of amplification by interaction between two electron streams. Bell Sys. Tech. J. 28: 52-8. 1949.

3. NERGAARD, L.S. Analysis of a simple model two-beam growing-wave tube. R.C.A. Rev. 9: 585-601. 1948.

4. PIERCE, J.R. and HEBENSTREIT, W.B. A new type of high frequency amplifier. Bell Sys. Tech. J. 28: 33-51. 1949.

5. PIERCE, J.R. Double-stream amplifiers. Proc. I.R.E. 37: 980-85. 1949.

6. PIERCE, J.R. Increasing space-charge waves. J. App. Phys. 20: 1060-66. 1949.

7. HOLLENBERG, A.V. The double-stream amplifier. Bell Lab. Rec. 27: 290-2. 1949.

8. SPANGENBERG, K.R. Vacuum tubes. McGraw-Hill Book Co., Inc., New York. 1948.

9. PIERCE, J.R. Theory and design of electron beams. D. Van Nostrand Co., Inc., New York. 1949.

10. HANLEY, T.E. Spectral emissivity and electron emission constants of thoria cathodes. J. App. Phys. 19:583. 1948.

11. BRONWELL, A.B. and BEAM, R.E. Theory and applications of microwaves. McGraw-Hill Book Co., Inc., New York. 1947.